Global Medical Genetics 13 (2026) 100094

Contents lists available at ScienceDirect

Global Medical Genetics

journal homepage: www.keaipublishing.com/en/journals/global-medical-genetics/

Cannabidiol modulates exosomal miRNA networks to enhance Imatinib mesylate response in chronic myelogenous leukemia

Petar Petrov Donchev [a,*], Evelina Yordanova Vasileva [b], Tsvetelina S. Paunova-Krasteva [a], Svetla Trifonova Danova [a]

[a] The Stephan Angeloff Institute of Microbiology, Bulgarian Academy of Sciences, 26 Acad. G. Bonchev Str., Sofia 1113, Bulgaria
[b] Faculty of Chemistry and Pharmacy, Sofia University "St. Kliment Ohridski", 1 James Bourchier Blvd., Sofia 1164, Bulgaria

ARTICLE INFO

Article history:
Received 26 November 2025
Received in revised form 15 January 2026
Accepted 15 January 2026
Available online 19 January 2026

Keywords:
Chronic myelogenous leukemia (CML)
Imatinib resistance
Cannabidiol (CBD)
Exosomal miRNAs
HMGB1 regulation

ABSTRACT

Background/Objectives: Chronic myelogenous leukemia (CML) is a clonal myeloproliferative disease driven by the BCR-ABL1 fusion oncogene. Tyrosine kinase inhibitors (TKIs) such as Imatinib mesylate have dramatically improved patient outcomes, yet resistance remains a major obstacle to long-term efficacy. Exosomes, as carriers of bioactive molecules including miRNAs, are increasingly recognized as mediators of drug resistance. CBD has demonstrated antiproliferative and pro-apoptotic effects in several cancer models, but its potential to modulate Imatinib sensitivity or resistance in CML remains unclear. This study aimed to investigate exosomal miRNA signatures associated with Imatinib sensitivity and resistance in the context of treatment with Cannabidiol (CBD), Imatinib mesylate (IM), and their combination.
Methods: Following treatment with CBD, IM, and CBD+IM, exosomal miRNA profiles in Imatinib-sensitive (K-562S) and Imatinib-resistant (K-562 R) cell lines were analyzed. Gene Ontology (GO) enrichment and semantic clustering was performed.
Results: CBD activated tumor-suppressive and apoptosis-related miRNAs in K-562S cells, whereas K-562 R cells showed a dual response involving oncogenic miRNAs and metabolic regulators. IM induced suppressive cascades in K-562S but caused loss of canonical tumor suppressors in K-562 R. CBD+IM produced synergistic amplification of apoptotic and differentiation-related pathways in sensitive cells, while resistant cells showed partial restoration of apoptosis but persistent loss of tumor suppressors. HMGB1-associated miRNAs were identified, of which suppressed were miR-615–5p, miR-4435, let-7 g-3p, and the miR-548 family, alongside upregulated miR-3191–3p and miR-33a-5p.
Conclusions: Circulating miRNAs are valuable biomarkers for TKI resistance in CML. Targeting HMGB1-associated miRNAs, together with combined CBD and IM treatment, may help re-establish apoptotic regulation and overcome resistance mechanisms.

Introduction

Chronic myelogenous leukemia (CML) is a clonal myeloproliferative neoplasm of the pluripotent stem cell bearing a genetic hallmark, the BCR-ABL1 fusion oncogene, which is a result of a reciprocal chromosomal translocation t(9;22)(q34;q11), called the Philadelphia chromosome [1]. The product of this gene, the Bcr-Abl oncoprotein, is a constitutive tyrosine kinase, which promotes uncontrolled proliferation, impaired apoptosis, and genomic instability in hematopoietic stem and progenitor cells [2]. Since the introduction of the first representative of the tyrosine kinase inhibitors (TKIs), Imatinib mesylate (IM), treatment outcomes in CML have improved dramatically, with most patients achieving sustained remission and overall survival close to the general population [3].

Abbreviations: CBD, Cannabidiol; IM, Imatinib; GO, Gene Ontology; KEGG, Kyoto Encyclopedia of Genes and Genomes; MDR1, Multidrug Resistance Protein 1; ABCB1, ATP Binding Cassette Subfamily B Member 1; MTT, 3–4,5-Dimethylthiazol-2-yl-2,5-Diphenyltetrazolium Bromide Assay; CI, Combination Index; DRI, Dose Reduction Index; PPI, Protein-Protein Interaction; MCODE, Molecular Complex Detection algorithm; DNBSEQ, DNA Nanoball Sequencing; FASTQ, Text-based format for sequencing reads; AASRA, Anchor Alignment-Based Small RNA Annotation; Rfam, RNA Families Database; OncomiRs, Oncogenic microRNAs; UpSet, Visualization method for intersecting sets; MOMP, Mitochondrial Outer Membrane Permeabilization; CLASH/HITS-CLIP, Crosslinking, Ligation, and Sequencing of Hybrids/High-Throughput Sequencing of RNA isolated by Crosslinking Immunoprecipitation

* Corresponding author.
E-mail address: petardonchev@yandex.com (P.P. Donchev).

https://doi.org/10.1016/j.gmg.2026.100094

However, a substantial number of patients develop resistance to Imatinib after prolonged therapy, which necessitates further investigation to better understand the underlying molecular mechanisms [4].

Imatinib resistance has been described as caused by both BCR-ABL1-dependent mechanisms, such as kinase domain mutations (e.g., T315I, M351T), gene amplification, and overexpression, and BCR-ABL1-independent pathways, including drug efflux, activation of alternative signalling cascades, and dysregulation of apoptosis autophagy [5,6]. Importantly, the increased expression of ATP-binding cassette transporter MDR1 (P-glycoprotein), encoded by the ABCB1 gene, is another resistance related process that leads to reduced intracellular drug accumulation and multidrug resistance in CML and many other malignancies [7,8].

Recently, the non-psychoactive cannabinoid, cannabidiol (CBD), has garnered attention for its anticancer potential. CBD has exhibited antiproliferative, pro-apoptotic, anti-inflammatory, and anti-angiogenic effects in a wide variety of experimental models [9,10]. CBD has also been shown to modulate the expression of the drug transporter P-glycoprotein and sensitize resistant cancer cells to chemotherapeutic agents [11,12]. These properties reveal CBD`s potential to influence mechanisms relevant to TKI response in CML, yet it putative role in modulating sensitivity or resistance to IM remains largely uknown. Additionally, CBD has been found to inhibit exosome and microvesicle release in cell lines from solid tumors, although this needs to be verified for hematological malignancies [13]. Studies have demonstrated CBD antitumor activity in multiple cancer models through induction of apoptosis, modulation of inflammatory signalling, and interference with metabolic pathways. However, its potential to modulate IM sensitivity or overcome Imatinib-associated resistance in CML remains underexplored.

Over the past decade, exosomes have gained attention due to their important role in the mediation of intercellular communication within the tumor microenvironment, thus also serving as facilitators of drug resistance [14,15]. Exosomes are nano-sized vesicles (30–150 nm) shed by most cell types, including cancer cells, and serve as a vehicle for bioactive molecules such as proteins, lipids, mRNAs, non-coding RNAs, and miRNAs [16]. Scientific studies have demonstrated that these vesicles facilitate the transfer of functional biomolecules to recipient cells, thereby influencing gene expression, altering signalling pathways, and contributing to drug resistance [17].

Given the selective miRNA content of exosomes, the functional roles of these miRNAs must be understood to properly interpret their contribution to drug resistance. miRNAs are small non-coding RNAs involved in regulating gene expression at the post-transcriptional level, and they have been implicated in diverse mechanisms of drug resistance, including modulation of apoptosis, cell cycle progression, and drug efflux [18]. Recent systematic analysis has summarized the available clinical data highlighting the importance of multiple miRNAs in TKI response and resistance [19]. Numerous studies have demonstrated that miRNAs found in exosomes derived from drug-resistant cancer cells can spread resistance in sensitive cells [20,21]. For instance, exosomes secreted by imatinib-resistant K-562 cells have been shown to contain high levels of MDR1 mRNA and specific miRNAs such as miR-125b-5p, miR-99a-5p, and miR-210–3p, which were previously found to regulate genes related to apoptosis, drug efflux, and stemness [22,23]. These findings demonstrate the vast potential of exosomal miRNAs as biomarkers and therapeutic targets in personalized medicine, which would allow for circumvention of therapeutic non-responsiveness or reversal of acquired tolerance. In CML specifically, exosomal miRNAs have been implicadted in IM resistance in both cell line models and patient plasma, demonstrating their relevance as mediators of drug response. A comprehensive evaluation of exosomal non-coding RNAs in leukemias additionally reinforces the relevance of exosomal-derived miNRAs as key modulators of therapeutic response [24]. Further, exosomal miRNAs mediate intercellular communication and have been implicated in drug resistance by transferring regulatory RNAs that modulate apoptosis, drug efflux, and immune interactions. In CML, several studies report altered exosomal miRNA signatures associated with imatinib resistance in cell models and patient plasma, implicating miRNAs that regulate BCL2 family members, ABC transporters, and signaling pathways such as PI3K/AKT. Nevertheless, a systematic comparison of exosomal miRNA changes between imatinib sensitive and resistant cells under CBD, IM, and combined treatment has not been reported.

Recent studies have provided evidence suggesting that microRNAs (miRNAs) may play a pivotal role in the modulation of cellular responses to tyrosine kinase inhibitor (TKI) therapy. In the context of CML, intrinsic and acquired resistance to Imatinib has been linked to changes in miRNA expression [25], often exerted through modulation of important signalling molecules and survival pathways [26]. Importantly, several miRNAs have been shown to modulate the expression levels and activity of high mobility group box 1 (HMGB1), a chromatin-binding protein involved in DNA repair, inflammation, and autophagy [27]. HMGB1 has emerged as a critical mediator of chemoresistance and cellular stress responses. Thus, its regulation by miRNAs may represent an underexplored pathway contributing to TKI resistance [28]. Understanding the interplay between miRNAs and HMGB1 offers the opportunity to uncover new therapeutic targets and improve current treatment strategies to overcome resistance in CML.

In this study, Imatinib-sensitive (K-562S) and Imatinib-resistant (K-562R) CML cell lines were used to investigate the effects of Imatinib mesylate (IM), cannabidiol (CBD), and their combination (IM+CBD) on exosomal miRNA profiles with the aim of identifying differentially expressed miRNAs potentially associated with treatment response or resistance. The observed results provide novel insights into the miRNA-related mechanisms of resistance and demonstrate CBD's potential to modulate exosomal signalling pathways, offering broader therapeutic strategies to overcome TKI resistance in CML.

Materials and methods

Cell lines and reagents

The Imatinib-sensitive human chronic myeloid leukemia cell line K-562S was purchased from Leibniz-Institut DSMZ, Braunschweig, Germany, while the Imatinib-resistant K-562R cell line was provided by Prof. Carlo Gambacorti-Passerini (Università degli Studi di Milano-Bicocca, Italy). Cells were cultured in RPMI-1640 medium (CAPRICORNTM) (with phenol red, without HEPES, without sodium pyruvate) supplemented with 10 % v/v fetal bovine serum (FBS) (Non-USA origin fetal bovine serum (SIGMA F9665) at 37 °C in a humidified atmosphere containing 5 % CO_2.

Imatinib mesylate (Sigma-Aldrich with CAS registry No.: 1020149-73-8) and cannabidiol (CBD) (Cayman Chemical with CAS registry No.: 13956-29-1) were dissolved in sterile distilled water and pure ethanol, respectively. Working concentrations were freshly prepared in culture medium prior to treatment.

Cytotoxicity and combination treatment assays

Cell viability was assessed using an MTT assay following drug treatment with Imatinib mesylate, CBD, or a combination of both agents. Cells were seeded in 96-well flat-bottom plates (100 μL/well) at maximum viable cell density (3×10^5 cells/well) in culture medium (RPMI 1640 supplemented with FCS 10 % v/v). After 24 h (37°C in humidified incubator containing 5 % CO2), cells were treated with gradient concentrations of Imatinib mesylate, CBD, or their

combination (IM+CBD) for 72 h. K-562S (Imatinib-sensitive) and K-562R (Imatinib-resistant) cells were exposed to a range of IM and CBD concentrations to determine dose-response relationships and to identify concentrations that elicit sublethal stress versus cytotoxicity. Substance concentrations were selected based on preliminary IC50 determinations for each cell line to ensure comparable biological perturbation across sensitivity states. After addition of 10 μL MTT dye (5 mg/mL in PBS), cells were further incubated for 4 h at 37°C. Then, the formed formazan crystals were resuspended by adding 100 μL of isopropanol with 5 % v/v formic acid to each well, and absorbance was measured at 570 nm using INNO microplate spectrophotometer (LTEK Co., Ltd., Gyeonggi-do, South Korea).

For combination treatment K-562S (Imatinib sensitive) and K-562R (Imatinib resistant) cells were seeded in fresh culture medium onto 96 well plates at a density of 3×10^5 cells per well. CBD and IM were applied in combination at fixed ratio concentrations. For K-562S cells, CBD was tested at 8, 16, and 24 μM, while imatinib was applied at 0.05, 0.1, and 0.2 μM. For K-562R cells, CBD was tested at 15, 20, and 25 μM, and IM at 1.2, 2.2, and 2.8 μM. After 72 h of exposure, antiproliferative activity was determined by MTT assay, and absorbance was measured with INNO microplate spectrophotometer (LTEK Co., Ltd., Gyeonggi-do, South Korea). Combination Index (CI) values were calculated according to the median effect (Fa) equation (Chou–Talalay method) using CompuSyn software (ComboSyn Inc.). CI values < 0.9 were interpreted as synergistic, between 0.9 and 1.10 as additive, and > 1.10 as antagonistic interactions.

Exosome isolation and RNA extraction

After 48 h of treatment, cells were separated from culture supernatants by preliminary centrifugation at 2000 rpm for 30 min. The resulting cell-free supernatants were then processed for exosome isolation using miRCURY Exosome Cell/Urine/CSF kit in accordance with the manufacturer`s protocol. MicroRNAs were extracted from exosomes using miRNAeasy Tissue/Cells Advanced kit, following the manufacturer`s instructions. The quality and quantity of miRNA were assessed with a Bioanalyzer, followed by NGS sequencing performed by BGI Genomics (Shenzhen, Guangdong, China).

Western blot analysis of exosomes

Exosomal protein expression was assessed by Western blotting analysis. Purified exosome preparations were lysed in RIPA buffer (Sigma Aldrich) supplemented with Protease and Phosphatase Inhibitor Cocktail (PPC1010, Sigma Aldrich). Protein concentrations were determined using a BCA assay, and equal amounts of protein (20–30 μg per lane) were resolved on hand cast polyacrylamide gels prepared with Acrylamide/Bis acrylamide solution (29:1; Cat. A2792 100 ML, Sigma Aldrich) and polymerized using TEMED (T9281, CAS No. 110 18 9, Merck/Sigma Aldrich) and ammonium persulfate. Proteins were transferred to PVDF membranes, which were blocked with 5% skim dry milk in TBST and incubated overnight at 4 °C with primary antibodies against Flotillin 1 (HY P80675, MedChemExpress) and CBD81 (MedChemExpress). After washing, membranes were incubated for 1 h at room temperature with HRP conjugated secondary antibody (HY P8004, AffiniPure Goat Anti Mouse IgG H&L, MedChemExpress). Protein bands were visualized using Clarity™ Western ECL Substrate (Cat. #170 5060, Bio Rad) and developed on a ChemiDoc imaging system (Bio-Rad, Hercules, CA, USA).

Dynamic light scattering of exosomes

Exosome size measurements were carried out using a NanoBrook 90Plus PALS analyzer (Brookhaven Instruments Corporation, Nashua, NH, USA) equipped with a 35 mW red diode laser operating at λ = 640 nm. Measurements were recorded at a fixed scattering angle (θ) of 90°, with all analyses performed at a controlled temperature of 25 °C. The hydrodynamic diameter, Dh, of the vesicles was obtained from the diffusion coefficients calculated by the instrument, applying the Stokes–Einstein equation.

Electron microscopy of exosomes

To assess the presence of exosomes, transmission electron microscopy (TEM) was performed using a negative-contrast staining technique. A volume of 10 μL of the isolated exosomes was deposited onto copper grids (300 mesh) for electron microscopy, previously coated with a thin Formvar film. The grids were incubated for 40 min at room temperature to allow adsorption of the exosomes onto the grid surface. The next step involved contrasting with a 1% uranyl acetate solution. Observations were carried out using a Transmission Electron Microscope HR STEM JEOL JEM-2100 (JEOL Ltd., Tokyo, Japan) operating at 200 kV, equipped with a CCD camera GATAN Orius 832 SC1000 (Gatan GmbH, Munich, Germany).

Small RNA sequencing, target prediction, and functional enrichment

Library preparation and sequencing: Exosomal small RNAs were subjected to strict quality control prior to library construction. Libraries were prepared by sequential adaptor ligation at the 3′ and 5′ ends, incorporation of unique molecular identifiers (UMIs), first and second strand synthesis, fragment selection, and cyclization. Libraries were quantified, pooled, and quality checked before sequencing on the DNBSEQ platform.

Data processing and filtering: Raw reads (49 nt) were processed to remove adaptors, low quality sequences, polyA contamination, and fragments < 15 nt. Clean tags were retained in FASTQ format and used for downstream analysis. Sequence length distribution was assessed to confirm enrichment of miRNAs (21–22 nt) and other small RNA classes.

Alignment and annotation: Clean reads were aligned to the human reference genome GRCh38 (GCF_000001405.39_p13) using Bowtie2 (allowing one mismatch). Non coding RNA annotation was performed with AASRA (no mismatches, variable length) and cmsearch against the Rfam database. Small RNAs were classified according to a hierarchical annotation priority (miRBase > piRNABank > snoRNA > Rfam > other sRNA). Unannotated fragments were used for novel miRNA prediction.

Target gene prediction: Target genes of both known and predicted miRNAs were identified using three independent prediction algorithms. Only interactions supported by at least two of the three software tools were retained to construct the final target gene dataset. All prediction results were available in the “miRNA Target” section of the Dr.Tom system, with parameter details provided in the Help Information.

Differential expression was assessed using multiple statistical frameworks provided by BGI, including DESeq2, DEGseq, and PossionDis. According to the analysis report, significantly differentially expressed miRNAs were defined using the following thresholds:DESeq2: $|\log2FC| > 0$ and Q-value ≤ 0.05; DEGseq / PossionDis: $|\log2FC| \geq 1$ and Q-value ≤ 0.001. Q-values represent Benjamini–Hochberg adjusted p-values. For downstream visualization and comparative interpretation in this study, a more stringent cutoff of $\log2FC \geq 2.0$ was applied to highlight robust expression changes across treatments and between K-562S and K-562R cells. Differentially expressed miRNAs identified under these criteria were used for target prediction, Gene Ontology enrichment, and network-based functional clustering as described in Sections 2.8–2.10.

Gene ontology and pathway enrichment analyses

A baseline functional enrichment of differentially expressed genes was performed by BGI Genomics using their standard analytical pipeline. Candidate genes were mapped to Gene Ontology (GO) terms (http://www.geneontology.org/) using the full human genome as background. Enrichment significance was assessed using a hypergeometric test implemented via the phyper function in R, followed by multiple-testing correction using the qvalue package. Only GO terms with a corrected Q-value ≤ 0.05 were considered significantly enriched. This analysis provided an overview of biological processes and pathways associated with the differentially expressed gene sets.

MCODE subnetwork detection and semantic GO clustering

To identify treatment-specific functional modules, we performed a second, network-focused enrichment workflow based on protein–protein interaction (PPI) subnetworks. Predicted target genes of differentially expressed exosomal miRNAs were queried against the STRING database (https://string-db.org) using a high-confidence interaction threshold (score ≥ 0.7) restricted to *Homo sapiens*. Resulting PPI networks were imported into Cytoscape (v3.x), filtered to remove low-degree nodes and edges, and clustered using the MCODE plugin with default parameters (degree cutoff = 5, node score cutoff = 0.7, k-core = 5, max depth = 3). The highest-scoring MCODE clusters were retained for functional annotation.

Each MCODE subnetwork was subjected to GO Biological Process enrichment using the enrichGO function from the clusterProfiler package (v4.x) with *org.Hs.eg.db* as the annotation database. Enrichment was performed using Benjamini–Hochberg correction, and GO terms with q ≤ 0.05 were considered significant. To reduce redundancy and group related GO terms into higher-order functional themes, semantic similarity analysis was conducted using GOSemSim (method = "Wang"). Pairwise similarity matrices were clustered using hierarchical clustering (average linkage) followed by dynamic tree cutting (dynamicTreeCut; deepSplit = 2, minimum cluster size = 5). Each semantic cluster was assigned an "AutoTheme" identifier, which was merged back into the enrichment results to generate treatment-specific functional themes.

Theme assignment was summarized at both the cluster and treatment levels, including term counts per theme and treatment × theme contingency matrices. Visualization of functional patterns included UpSet plots (UpSetR) to assess gene overlap across treatments and themes. All analyses were performed in RStudio (v4.x) using clusterProfiler, org.Hs.eg.db, dplyr, GOSemSim, dynamicTreeCut, UpSetR, tidyr, and ggplot2.

Annotation and visualization of HMGB1-associated miRNAs

HMGB1-associated miRNAs were retrieved using multiMiR R package, which aggregates experimentally supported and predicted miRNA-target interactions. multiMiR R package, which aggregates experimentally supported and predicted miRNA-target interactions was used to retrieve HMGB1-associated miRNAs. Differential expression values (log2FC and adjsuted p-values) for these miRNAs were extracted from DESeq2 analysis of K-562S and K-562R cells. A unified evidence category was generated by merging evidence annotation from multiMiR with the expression data and thereafter collapsed per miRNA. Heatmaps with hierarchical clustering were produced with evidence types displayed as row annotations.

Results

Comparative antiproliferative effects of IM and CBD in parental and resistant K-562 cells

K-562S and K-562 R cells were exposed to varying concentrations of IM or CBD for 72 h, followed by MTT cell growth assay to evaluate inhibition of cell proliferation (Fig. 1). To maintain the resistant phenotype, prior to treatment, Imatinib-resistant K-562R cells were seeded in the presence of 1 μmol/L IM. Following treatment with IM a dose-dependent reduction in proliferation of K-562S cells was observed with highest inhibition at the maximum tested concentration (1 μmol/L) and an average IC_{50} value of 0.116 μmol/L. In contrast, even at higher Imatinib concentrations K-562R cells showed only partial inhibition, with an average IC_{50} of 2.88 μmol/L.

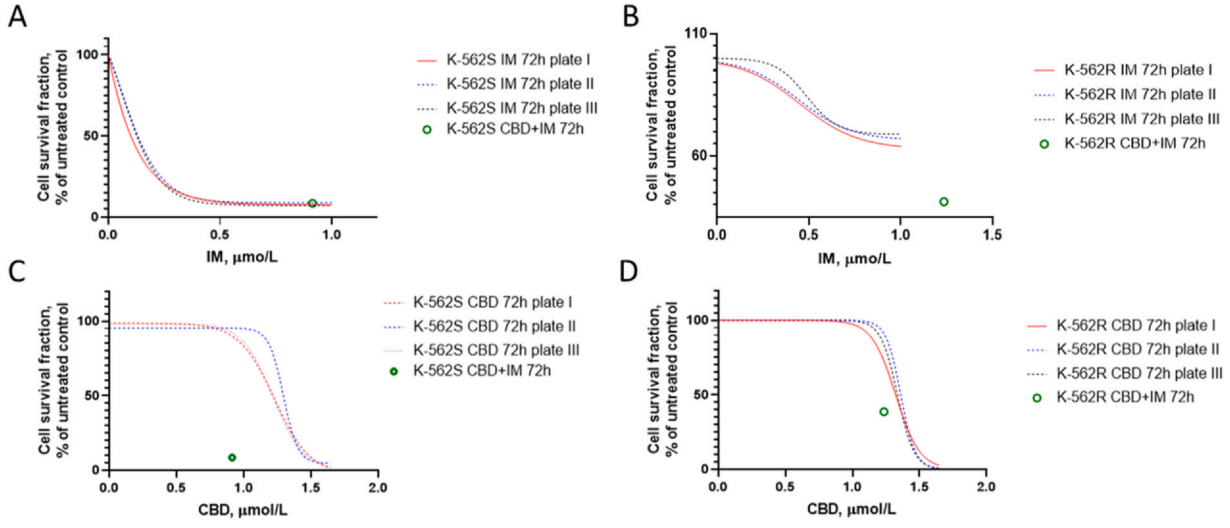

Fig. 1. Dose–response curves of K-562S (Imatinib-sensitive) and K-562 R (Imatinib-resistant) cells following 72 h exposure to varying concentrations of Imatinib (IM) or Cannabidiol (CBD), assessed by MTT cell growth assay. Only miRNAs shared across all three treatment conditions are displayed to highlight common regulatory patterns. K-562 R cells were maintained in 1 μmol/L IM prior to treatment to preserve the resistant phenotype. IM induced a dose-dependent inhibition of proliferation in K-562S cells, with maximal inhibition at 1 μmol/L and an average IC_{50} of 0.116 μmol/L (Fig. 1B), whereas K-562 R cells exhibited only partial inhibition with an average IC_{50} of 2.88 μmol/L (Fig. 1A). CBD treatment reduced proliferation in both cell lines, achieving up to 95.8 % inhibition in K-562S cells (IC_{50} = 17.69 μmol/L) (Figs. 1D) and 91.3 % inhibition in K-562 R cells (IC_{50} = 21.87 μmol/L) (Fig. 1C). These findings demonstrate that, despite resistance to IM, K-562 R cells remain sensitive to CBD, which exerts a consistent dose-dependent antiproliferative effect in both parental and resistant phenotypes.

Table 1
CI values of CBD in combination with IM on sensitive (K-562S) and resistant (K-562R) cells.

1 A					1B				
K-562S					**K-562R**				
IM (μM/L)	**CBD (μM/L)**	**Fa**	**CI**	**Interpretation**	**IM (μM/L)**	**CBD (μM/L)**	**Fa**	**CI**	**Interpretation**
0.05	8.0	0.55	1.23	Antagonism	1.6	15.0	0.23	0.73	Synergy
0.05	16.0	0.25	1.23	Antagonism	1.6	20.0	0.14	0.73	Synergy
0.05	24.0	0.11	1.06	Additive	1.6	25.0	0.12	0.82	Synergy
0.10	8.0	0.27	0.65	Synergy	2.2	15.0	**0.20**	**0.69**	**Synergy (chosen dose)**
0.10	16.0	0.11	0.73	Synergy	2.2	20.0	0.15	0.77	Synergy
0.10	24.0	0.10	1.04	Additive	2.2	25.0	0.13	0.86	Additive
0.20	**8.0**	**0.12**	**0.39**	**Strong synergy (chosen dose)**	2.7	15.0	0.24	0.79	Synergy
0.20	16.0	0.25	1.23	Antagonism	2.7	20.0	0.19	0.86	Synergy
0.20	24.0	0.11	1.06	Additive	2.7	25.0	0.15	0.96	Synergy
Fixed-ratio concentrations		**K-562S (IM:CBD=1:160)**			**Fixed-ratio concentrations**		**K-562R (IM:CBD=1:9)**		
Total Dose (μM)		**Fa**	**CI**	**Interpretation**	**Total Dose (μM)**		**Fa**	**CI**	**Interpretation**
8.20 (0.2 +8)		**0.12**	**0.39**	**Strong synergy**	**17.20 (2.2 +15)**		**0.20**	**0.69**	**Synergy**
16.05		0.25	1.23	Antagonism	21.6		0.14	0.73	Synergy
24.05		0.11	1.06	Additive	26.6		0.12	0.82	Synergy

CBD treatment demonstrated antiproliferative effects in both cell lines. In K-562S cells, CBD reduced proliferation by up to 95.8 % at 44.0 μmol/L, with an average IC_{50} of 17.69 μmol/L. Similarly, in K-562S cells, CBD achieved a maximum inhibition of 91.3 % at 44.0 μmol/L, with an average IC_{50} of 21.87 μmol/L. Together, these results indicate that despite the resistance to IM, K-562R cells remain sensitive to CBD, which exerts consistent dose-dependent antiproliferative effect in both parental and resistant phenotypes.

Synergy assessment

The interaction between CBD and IM was evaluated by calculating CI using CompuSyne software. The response to the combined treatment in K-562S cells was found to be heterogeneous and included antagonistic effects at certain dose levels (e.g., 0.05 μM IM + 16 μM CBD, CI ≈ 1.23)(Table 1A), whereas strong synergy was found at the clinically relevant combination of 0.2 μM IM + 8 μM CBD (Fa = 0.12, CI = 0.39). In contrast, the concomitant treatment in K-562R cells exerted a more uniform effect, with CI values consistently found in the synergistic range (0.69–0.82)(Table 1B). Of particular interest was the combination of 2.2 μM IM + 15 μM CBD, which demonstrated effective re-sensitization of resistant cells to IM by CBD treatment. The findings above indicate that synergy in sensitive cells is dose-dependent, whereas CBD co-treatment demonstrated consistent therapeutic advantage in the resistant cell line.

Dose optimization and reduction index

The dose-sparing effect achieved by the combined treatment was measured using the dose reduction index (DRI). In K-562S cells, the combination of 0.2 μM IM + 8 μM CBD produced 5.89 DRI for IM and 4.52 DRI for CBD, showing that the observed effect is accompanied by a substantial dose reduction of the applied substances (Table 2A). In K-562R cells, the combination of 2.2 μM IM + 15 μM CBD yielded an even greater impact, with DRI of 9.18 for IM and 1.72 for CBD (Table 2B). Over the range of the tested concentrations, the combined treatment in resistant cells produced consistently higher DRI values for IM, which is strong evidence in favor of CBD`s chemosensitizing role in overcoming resistance. Collectively, these results validate the therapeutic potential of CBD to increase sensitivity to IM while also limit the unnecessary drug burden, particularly in resistant leukemia cases.

Immunoblot confirmation of exosomal proteins

To identify the exosomal protein markers EVs from K-562S and K-562R cells were subjected to Western blotting analysis. All samples consistently expressed Flotillin-1 and CD81, confirming their extracellular vesicle origin. The presence of these constitutive markers in all treatment conditions (Control, IM, CBD, CBD+IM) and cell lines is robust confirmation of the successful isolation of exosomes devoid of contaminating non-vesicular proteins (Fig. 2). No major differences in marker expression were detected between treatments, indicating that drug exposure did not compromise exosome integrity.

Size distribution of exosomes by dynamic light scattering

Dynamic light scattering analysis confirmed that all preparations contained vesicles within the expected exosomal size range (Table 3) (Fig. 3). The mean hydrodynamic diameters of K-562R-derived vesicles ranged from 31.2 nm (Control) to 43.2 nm (CBD), with corresponding PDIs indicating moderately uniform populations. Across both phenotypes, CBD and IM demonstrated tendency to increase the average particle diameter relative to untreated controls, whereas the combination treatment produced more variable effects. A representative DLS size-distribution histogram is shown.

TEM

The presented electron microscopy micrographs demonstrate the presence of spherical exosomes isolated from K-562R and K-562S cells (Fig. A, B – white arrows). Exosomes isolated from the K-562R

Table 2
DRI values of CBD and IM on CML cells at a fixed ratio (K-562S, 1:160) and (K-562R, 1:9).

2 A					2B				
K-562S					**K-562R**				
Fa	**Dose IM**	**Dose CBD**	**DRI IM**	**DRI CBD**	**Fa**	**Dose IM**	**Dose CBD**	**DRI IM**	**DRI CBD**
0.12	0.20	8.0	5.89	4.52	0.12	2.70	25.0	9.98	1.39
0.25	0.172	24.65	1.73	1.55	0.20	2.20	15.0	9.18	1.72
0.55	0.077	13.79	1.54	1.72	0.23	1.60	15.0	8.05	1.66

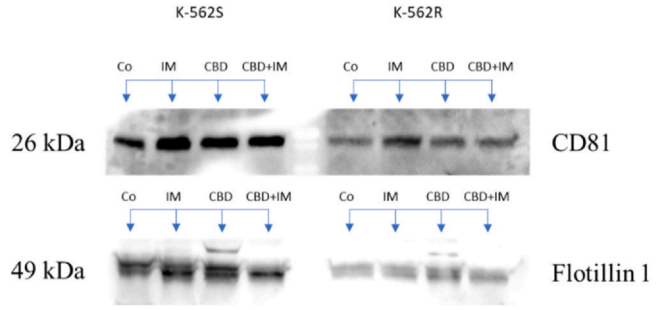

Fig. 2. Immunoblot confirmation of exosomal markers in K-562S and K-562R cells. Western blot analysis of exosomal proteins isolated from K-562S (left panel: Control, IM, CBD, CBD+IM) and K-562R (right panel: Control, IM, CBD, CBD+IM) cells. Membranes were probed with antibodies against Flotillin 1, CD81, and Transferrin receptor 1 (TfR1). All preparations showed positive expression of exosomal markers, confirming vesicle identity across treatments.

Table 3
Hydrodynamic Diameter (Dh) of exosomes isolated from K-562S and K-562 R cells under different treatment conditions.

Sample	Dh*, nm	± SD
1 K-562R Control exosomes	31.2	5.6
2 K-562R CBD exosomes	43.2	7.1
3 K-562R IM exosomes	34.3	4.9
4 K-562R CBD+IM exosomes	40.3	9.1
5 K-562S control exosomes	39.8	7.8
6 K-562S CBD exosomes	44.9	8.3
7 K-562S IM exosomes	51.1	10.2
8 K-562S CBD+IM exosomes	33.4	3.8

cell line range in size between 30–40 nm. With respect to their morphology, the presence of an outer, electron-dense, structurally defined membrane can be observed (Fig. 4, A). The sample derived from the K-562S cell line includes exosomes with sizes ranging from 20 to 30 nm (Fig. 4, B), arranged in clusters.

miRNA differential expression analysis

The differential expression analysis following treatment with CBD, IM, and their combinations revealed distinct exosomal miRNA signatures in Imatinib-resistant (K-562R) and imatinib-sensitive (K-562S) cells. The majority of differentially expressed miRNAs found in the exosomes under all treatment conditions (CBD, IM, combination) exhibited log2 fold change well above 4, with many exceeding 20. The magnitude of these changes signifies strong transcriptional or post-transcriptional regulation in response to the treatment, potential identification of biomarker candidates for resistance or sensitivity, and possibilities for additional downstream pathway enrichment and network analysis (Fig. 5 and Table 4).

Experimental assessment of exosomal differential miRNA expression

K562-R cell line

•CBD Treatment: dual induction of tumor suppressors and OncomiRs in K-562R cells

In K-562R cells, treatment with CBD produced a complex exosomal miRNA expression profile, characterized by simultaneous induction of tumor-suppressive and oncogenic regulators. Among the most prominent changes was the strong upregulation of the poorly characterized miRN-4463, which may be linked to apoptosis and oxidative stress. Several canonical tumor-suppressive miRNAs were also overexpressed, including miR-29b-3p and miR-29c-3p, which regulate DNA methylation and apoptosis pathways, as well as miR-101–3p, a known inhibitor of EZH2 and BIRC5. At the same time, CBD also induced strong expression of oncogenic miRNAs, including miR-21–3p, a regulator of PTEN/PI3K/AKT and NF-κB signalling, and miR-

Table 4
Comparative Highlights of Exosomal miRNA Responses in Resistant (K-562R) and Sensitive (K-562S) Cells.

miRNA	K-562 R Response	K-562S Response	Pathway / Functional Category	Shared / Contrasting Behavior
miR-3191–3p	↑ (CBD, IM, CBD+IM)	↓↓↓ (IM)	Stress-adaptation, radioresistance	Strongest opposite regulation; resistance marker
miR-615–5p	↓↓↓ (all treatments)	–	Apoptosis, IGF2/AKT, mTOR	Consistent suppressor loss in resistance
let-7 g-3p	↓↓↓ (IM, CBD+IM)	–	Tumor suppression, RAS/HMGA2	Persistent loss of canonical suppressor in resistance
miR-4435	↓ (all treatments)	↓ (CBD+IM)	Context-dependent oncogenic/EMT	Consistent suppression; leukemia-specific behavior
miR-29b-3p / miR-29c-3p	↑ (CBD)	–	Apoptosis, DNA methylation	CBD-induced suppressors only in resistant cells
miR-101–3p	↑ (CBD)	–	EZH2/BIRC5 inhibition, apoptosis	Tumor suppressor induced only in resistant cells
miR-21–3p	↑ (CBD)	–	Oncogenic, PI3K/AKT, NF-κB	Stress-buffering oncogenic response unique to resistance
miR-362–3p/5p	↑ (CBD)	–	NF-κB / STAT3 activation	Oncogenic inflammatory signalling in resistance
miR-204–3p	↑ (CBD+IM)	–	Apoptosis, BCL2 targeting	Combination-specific apoptotic rescue in resistance
miR-1226–3p	↑ (CBD+IM)	↑ (IM)	Apoptosis, BCL2 inhibition	Shared apoptotic activation; stronger in K-562S
miR-103a-3p / miR-103a-2–5p	↑ (CBD)	↑↑ (IM)	Metabolism, AMPK, apoptosis	Shared metabolic/apoptotic regulator; stronger in K-562S
miR-200c-3p	↑ (CBD, CBD+IM)	–	EMT, oxidative stress	EMT/stress induction unique to resistant cells
miR-500a-3p / 5p	↑ (CBD, IM)	↑ (IM)	Necroptosis attenuation, oxidative stress	Shared family; treatment-dependent differences
miR-1–3p	–	↑↑↑ (CBD+IM)	Differentiation, apoptosis	Sensitive-specific lineage/apoptotic activation
miR-133a-3p / miR-133–3p	–	↑↑ (IM, CBD+IM)	Apoptosis, BCL2 inhibition	Sensitive-specific apoptotic signature
miR-122–3p	–	↑↑↑ (CBD+IM)	Metabolism, lipid regulation, apoptosis	Sensitive-specific metabolic/apoptotic activation
miR-5010–5p	↓ (CBD+IM)	↑↑ (IM)	Inflammation, PPP2R2D	Opposite regulation; inflammation-linked divergence
miR-1304–5p	↓↓↓ (CBD+IM)	–	Immune evasion, PD-L1 axis	Immune-linked suppression unique to resistance
miR-181d-5p	↓ (CBD+IM)	–	Immune regulation, cholesterol metabolism	Immune/metabolic regulator suppressed only in resistance
miR-3176	↓ (CBD+IM)	–	Metabolism, glucose regulation	Metabolic adaptation marker suppressed only in resistance
miR-1273 h-5p	↓ (CBD+IM)	–	Stress-response, oxidative stress	Stress-response miRNA suppressed only in resistance

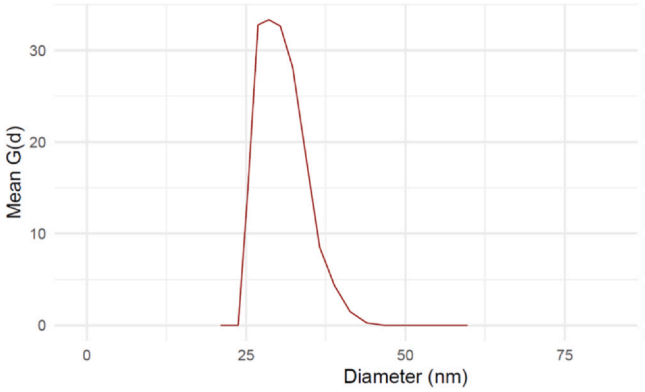

Fig. 3. Representative DLS size-distribution profile of isolated exosomes (0–100 nm).

362–3p/5p isoforms, which are associated with NF-κB and STAT3 activation in CML. Importantly, the observed upregulation of the metabolic regulator miR-33a-5p, which is involved in cholesterol transport and AMPK signalling, suggests that resistant cells may adapt to CBD treatment through metabolic pathway reprogramming. On the contrary, the sharp silencing of the tumor-suppressive miR-615–5p, described to be targeting IGF2 and AKT, indicate possible persistent pro-survival bias. Together, these findings indicate that CBD exerts a dual response in K-562R cells by simultaneously activating stress-induced tumor suppressors while maintaining oncogenic signalling.

The treatment with CBD altered several additional miRNAs implicated in diverse regulatory networks. For instance, miR-3529–3p and miR-103a-2–5p, both associated with stress and apoptosis regulation, were induced. The former is linked to vascular inflammation and stress-induced remodeling, while the latter is reported to be part of pro-apoptotic activity and oxidative stress modulation in AML cells. Additionally, elevated expression was observed for the members of the miR-200 family such as miR-141–3p and miR-200c-3p, which are linked to tumor-stroma interactions, oxidative stress regulation, and could also serve as prognostic markers in solid tumors. The passenger strands miR-17–3p and miR-19b-1–5p, part of the miR-17–92 cluster, were upregulated too. These two miRNAs represent the oncogenic potential of that cluster through effects on proliferation, invasion, immune evasion, and inflammatory persistence. Moreover, the induction miR-374a-5p in that treatment delineates oncogenic and stress-responsive signals that have been associated with promotion of proliferation and migration in gastric and osteosarcoma models. Lastly, miR-500a-3p and miR-500a-5p, representatives of miR-500 family and known contributors to the necroptosis attenuation, oxidative stress regulation, and prevention of epithelial-mesenchymal transition were also upregulated.

•IM treatment: stress-adaptive induction during widespread loss of tumor suppressors

In resistant cells, IM triggered broad remodeling of exosomal miRNA cargo. Several stress-related miRNAs were strongly induced, including miR-1226–5p, which has been reported to promote proliferation and radioresistance through IRF1 suppression, and miR-3191–3p, which displayed opposite regulation compared to the IM-sensitive cells, suggesting a potential role as a resistance associated marker. However, these changes were outweighed by the loss of the tumor-suppressor let-7g-3p. Although our dataset revealed significant downregulation of the 3p strand, the canonical tumor-suppressive activity of the let-7 family has been primarily attributed to the 5p strands, highlighting a potentially underexplored role of let-7g-3p in regulating oncogenic targets such as RAS and HMGA2. Additional reduced suppressive miRNAs included miR-429, an established EMT suppressor, as well as miR-532–3p and selected members of miR-548 family, which have reported to exert tumor-suppressive activity in specific context. In contrast, miRNAs such as miR-106b-5p and miR-191–3p, commonly described as oncogenic, were downregulated, along with miR-1255a, for which emerging evidence suggests tumor-promoting activity. Overexpressed but poorly characterized miRNAs with prognostic potential for the resistant phenotype in CML included miR-3619–3p, miR-3667–5p, miR-5004–3p, miR-597–3p, and miR-616–5p. This pattern indicates that, although resistant cells initiate a stress-adaptive response through selective induction of miRNAs, the prevailing effect of IM treatment is the inhibition of tumor-suppressive networks, which in turn could contribute to strengthened resistance.

IM treatment modulated multiple additional exosomal miRNAs with heterogeneous regulatory effects. The two poorly characterized strands of miR-1273h (3p and 5p) implicated in oxidative stress responses and suppression of CXCL12, which possess potential roles in epithelial protection and inhibition of gastric cancer were downmodulated. Importantly, miR-1284, a reported HMGB1 inhibitor and suppressor of proliferation and migration in osteosarcoma was also downregulated. Conversely, the upregulation of miR-141–3p, a known EMT regulator and modulator of tumor–stroma interactions (and member of the miR-200 family), may be an indication to a treatment related contribution to metastatic niche formation. Several other miRNAs with limited functional annotation demonstrated marked regulation. Namely, miR-3126–5p was strongly repressed. Its predicted targets include chromatin regulators (HDAC1, TET2, MECP2) and signaling molecules (CXCL12, VEGFA), justifying further investigation of that miRNA. Despite limited experimental validation data, the robust upregulation of miR-3191–3p suggests potential significance for the K-562 cell phenotype. Among the most strongly downregulated miRNAs (log2FC - 21.55, adjusted $p = 1.26 \times 10–6$) was miR-3605–3p, which, according to database predictions, may play a role in extracellular signalling.

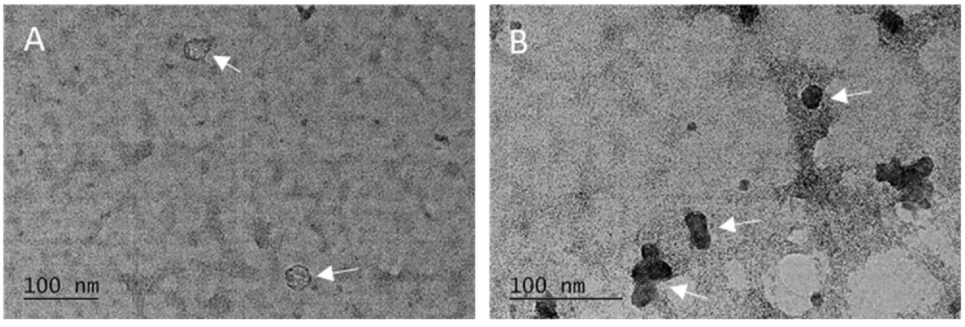

Fig. 4. Transmission electron microscopy of exosomes isolated from K-562 R and K-562S cells. Representative TEM micrographs show spherical extracellular vesicles consistent with exosomes (white arrows). K-562R–derived exosomes display diameters of approximately 30–40 nm and exhibit a well-defined electron-dense membrane. Exosomes isolated from K-562S cells are smaller (20–30 nm) and frequently appear in clustered arrangements.

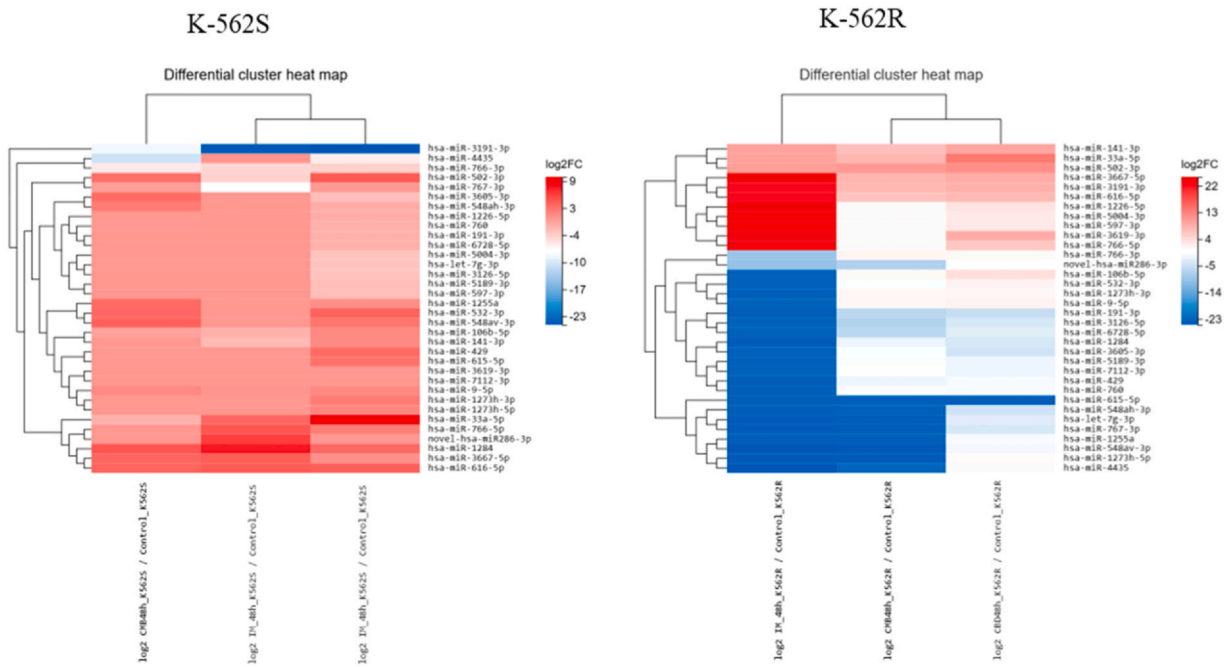

Fig. 5. Differentially expressed exosomal miRNAs in Imatinib sensitive (K-562S) and Imatinib resistant (K-562R) cells. Complete lists of differentially expressed miRNAs, including those unique to individual treatments, are provided in Supplementary Tables S1–S6. (a) Heatmap of exosomal miRNAs derived from K-562S cells following 48 h treatment with Imatinib mesylate (IM), cannabidiol (CBD), or their combination (CMB = CBD+IM). Differential expression is shown as log2 fold change (log2FC) relative to untreated controls, with significance defined at Benjamini–Hochberg-adjusted $p \le 0.05$. Samples: log2 IM_48h_K562S/Control_K562S, log2 CMB_48h_K562S/Control_K562S, log2 CBD_48h_K562S/Control_K562S. (b) Heatmap of exosomal miRNAs derived from K-562R cells following 48 h treatment with IM, CBD, or CMB. Differential expression is shown as log2FC relative to untreated controls, with Benjamini–Hochberg-adjusted $p \le 0.05$. Samples: log2 IM_48h_K562R/Control_K562R, log2 CMB_48h_K562R/Control_K562R, log2 CBD_48h_K562R/Control_K562R. Color scale indicates relative up or down regulation of miRNAs, highlighting distinct treatment dependent expression patterns between sensitive and resistant phenotypes.

Additional set of miRNAs with more established functions were also modulated. For instance, the reported CDK6 targeting cell cycle regulator miR-502–3p, known to exert tumor-suppressive activity in gastric and colorectal cancer was found to be upregulated. On the contrary, the suppression of miR-5189–3p suggests a loss of anti-proliferative control via EIF5A2 inhibition, as previously described in laryngeal carcinoma. Interestingly, miR-615–5p, described in the literature as tumor-suppressive via IGF2 and AKT2/LARP1-mTOR signalling, was downregulated. Moreover, the insufficiently characterized miR-6728–5p (log2FC −21.54, adjusted $p = 1.26 \times 10-6$) and miR-7112–3p (log2FC −21.64, adjusted $p = 1.26 \times 10-6$), with predicted roles in stress-related pathways and cellular signalling processes, were profoundly repressed.

In contrast to the miRNAs with insufficient experimental evidence, several miRNAs with established tumor-suppressive functions were consistently repressed. Among these, the downregulation of miR-760, previously linked to glioma invasion through MMP2 modulation and colorectal tumorigenesis, was evident. In addition, strand-specific regulation was observed for miR-766. The suppression of the NF-κB inhibitor miR-766-3p, which exerts anti-inflammatory activity, contrasted with marked upregulation of its alternative form, miR-766-5p, consistent with evidence that this variant may promote tumor progression. In line with these observations, suppression of miR-767-3p, downregulated in our dataset, has been described to enhance HIF1A signaling and metabolic adaptation in bladder cancer. Likewise, repression of the validated radiosensitizer miR-9-5p, which targets HK2, points to impaired apoptotic responses. Finally, the novel miR-286-3p, not yet functionally annotated in humans, was also downregulated. Drosophila analogs implicate miR-286 in JNK-mediated apoptosis-induced proliferation, suggesting a potential but as yet untested role for this miRNA in human biology.

•CBD+IM: partial restoration of apoptotic signalling but persistent suppressor loss

The combined CBD+IM treatment elicited a distinct exosomal miRNA profile, characterized by the induction of apoptosis-related miRNAs together with persistent downregulation of tumor suppressors. Notably, partial restoration of apoptotic signalling was evident through the strong upregulation of miR-204–3p, a direct BCL2 regulator and tumor suppressor. Evidence for stress-adaptive responses was provided by the induction of cell cycle-related miRNAs, including miR-107, miR-138–5p, and miR-3689b-5p. In addition, miR-4714–3p, whose function remains putative and requires further validation, was also strongly induced. This miRNA has been reported to target RTP4, a gene involved in immune response modulation and receptor trafficking. Altered RTP4 expression has been linked to disease states such as refractory primary biliary cholangitis, suggesting a potential role of miR-4714–3p in immune regulation. Furthermore, moderate upregulation of miR-200c-3p, miR-210–3p, and miR-501–3p indicates possible involvement in epithelial-to-mesenchymal transition (EMT), hypoxia responses, and apoptosis regulation, respectively. Nevertheless, CBD+IM treatment failed to restore several key tumor-suppressive miRNAs, including let-7 g-3p, miR-1225–5p, and miR-153–3p. In addition, miR-4435, reported as oncogenic in solid tumors but suppressed in our leukemia model, and miR-3121–3p, reported to promote tumor invasion and metastasis, both remained downregulated. Overall, the persistent loss of the let-7 family and other suppressive miRNAs demonstrates that although the combined treatment successfully reactivated apoptotic signalling through specific miRNAs, it does not completely overcome the resistant phenotype.

Beyond these canonical regulators, the combined treatment also altered a diverse set of exosomal miRNAs with emerging or context-specific roles. Among them were miR-10527–5p and miR-1293, which remain relatively undercharacterized. Sporadic reports implicate miR-10527–5p as an emerging cancer regulator (e.g., ESCC via Wnt/β-catenin), while miR-1293 appears to exert context-dependent

functions, acting as a tumor promoter in some cancers and a suppressor in others. Several miRNAs linked to metabolism and stress-related pathways were consistently downregulated. Of these, miR-1255a has been reported as a therapeutic target in breast cancer. miR-3176 (log2FC −21.80, adjusted $p = 2.45 \times 10^{-8}$) has been associated with glucose metabolism regulation in pancreatic β-cells, suggesting possible metabolic adaptation. Similarly, miR-1273 h-5p, a paralog of the stress-responsive 3p strand, was markedly downregulated (log2FC −22.05, adjusted $p \approx 7.13 \times 10^{-7}$). Although insufficiently characterized in cancer biology, this miRNA has been reported to protect corneal epithelial cells against UV-induced oxidative stress and apoptosis, suggesting that its downregulation may impair stress-response modulation.

Immune-related miRNAs were also affected. Notably suppressed was miR-1304–5p (log2FC −21.70, adjusted $p = 8.47 \times 10^{-7}$), which has been implicated in cisplatin resistance and immune evasion in NSCLC via the PD-L1 axis. Likewise, miR-181d-5p, a member of the miR-181 family, has been reported to influence T-cell regulation, cholesterol metabolism, and tumor suppression via MALT1 inhibition. Its downregulation here may reflect immune reprogramming, consistent with prior associations in autoimmune and metabolic disorders. Lastly, although less studied, miR-2110 (log2FC −2.21) has been proposed as a biomarker for brain ageing and autophagy-related processes.

Additional miRNAs with roles in development and differentiation were suppressed. These included the poorly characterized miR-25–5p (log2FC −20.94; adjusted $p = 4.36 \times 10^{-8}$), which may share functions with its paralog miR-25–3p, reported to promote cell cycle progression, invasion, and ER stress adaptation in colon cancer. miR-30d, secreted by the human endometrium and taken up by pre-implantation embryos, has been implicated in implantation signalling. Members of the miR-30 family, including miR-30d, have also been linked to adipocyte development, suggesting broader roles in differentiation and metabolic regulation. The poorly annotated miR-3605–5p and miR-3689e showed profound repression, which may indicate involvement in uncharacterized stress-responsive or epigenetic pathways.

Several miRNAs with inflammatory or fibrotic associations were also downregulated. These included miR-3939 and miR-3944–3p, for which target prediction suggests roles in inflammation and fibrosis, including hepatic gamma-glutamyl transferase activity for miR-3944–3p. The strongly repressed miR-5010–5p (log2FC −21.70, adjusted $p = 8.47 \times 10^{-7}$) has been shown to ameliorate high-glucose-induced inflammation via PPP2R2D modulation in renal cells, suggesting that its suppression here may diminish anti-inflammatory potential in leukemia.

Conversely, miR-502–3p was elevated. This miRNA has been reported to act as a tumor suppressor in several cancers through cell cycle regulation, and has also been proposed as a biomarker in Alzheimer's disease. In contrast, miR-509–3p, which has context-dependent roles across cancers, was profoundly repressed. While in colorectal cancer it has been reported to act oncogenically by targeting the tumor suppressor PHLPP2, its downregulation here may indicate loss of tumor-suppressive activity, consistent with observations in renal and ovarian cancer.

Members of the primate-specific miR-548 family (miR-548ah-3p and miR-548av-3p) and miR-550a-5p were also strongly downregulated. Whereas the former have been linked to immune tolerance and ovarian follicle activation, the latter has been reported to act oncogenically in lung adenocarcinoma by targeting LIMD1, suggesting that its downregulation here may relieve LIMD1 inhibition and contribute to anti-tumor signalling in leukemia cells.

Finally, both strands of miR-615 were suppressed, with miR-615–3p reported to regulate mitochondrial function and dentinogenesis, and miR-615–5p known to inhibit cervical and colorectal cancer progression via TMIGD2 and LARP1/mTOR pathways. Among other miRNAs, the strongly repressed miR-767–3p (log2FC −21.84; adjusted $p = 7.94 \times 10^{-7}$) has been reported to exert oncogenic effects in bladder cancer by enhancing HIF1A signalling and metabolic adaptation. Its downregulation here may reflect loss of such metabolic support in leukemia cells. Although poorly annotated in humans, miR-286–3p was moderately repressed (log2FC −7.22; adjusted $p = 0.0045$). Its Drosophila analogs are implicated in JNK-mediated apoptosis-induced proliferation, suggesting that its suppression may reduce stress-responsive proliferative signalling.

Together, these findings underscore the multifaceted nature of the combined treatment, which reactivates select apoptotic and metabolic regulators but fails to fully restore tumor-suppressive networks.

K562-S cell line

•CBD alters exosomal miRNA cargo with tumor-suppressive potential in K-562S

In Imatinib-sensitive K-562S cells, exposure to CBD elicited a pronounced remodeling of exosomal miRNA expression, characterized by the induction of miRNAs associated with apoptosis, differentiation, and cellular stress. Among the most strongly upregulated were miR-299–3p and miR-92b-5p, both exceeding 22 logFC, demonstrating robust activation. Previous research has implicated miR-299–3p in tumor suppression and cell cycle regulation, while miR-92b-5p has been linked to differentiation, stress adaptation, and apoptosis regulation. The miR-103a-3p, associated with metabolic and apoptotic regulation, was also strongly induced, potentially revealing CBD's effect on cellular energy homeostasis. Additionally, the upregulation of miR-34a-5p, a tumor suppressor that targets BCL2, together with miR-1226–3p, reported to promote apoptosis, further supported the activation of apoptotic signalling. Compared with resistant K-562R cells, sharp downregulation of miR-3191–3p was observed, suggesting its potential application as a biomarker of IM sensitivity. Collectively, these findings indicate that CBD promotes a pro-apoptotic and differentiation-stimulating exosomal miRNA profile, which is distinct from the mixed oncogenic and tumor-suppressive response observed in K-562R cells.

•IM: broad activation of tumor suppressors and stress-responsive miRNAs

The treatment with IM in K-562S cells resulted in prevalent upregulation of miRNAs related to tumor suppression and stress adaptation favoring apoptosis and cell cycle arrest. Among the most highly induced (log2FC > 21) were miR-133a-3p, miR-3173–5p, and miR-5010–5p. While miR-133a-3p is generally recognized as a tumor suppressor linked to differentiation and growth inhibition, miR-3173–5p has shown context-dependent roles in cancer progression, with both oncogenic and tumor-suppressive activities reported. In contrast, miR-5010–5p has been associated with reduced high-glucose-induced inflammation, suggesting its context-dependent protective role. miR-103–2–5p and miR-3194–3p were also strongly upregulated, possibly revealing involvement in modulation of metabolic and epigenetic regulators. In addition, the induction of miR-548e-3p and miR500a-3p, which are often found to be silenced in resistant cells, suggests partial restoration of tumor-suppressive signalling counteracting oncogenic networks. Moreover, miR-1226–3p showed moderate activation, which is in alignment with its reported role in BCL2 regulation and apoptosis promotion. Conversely, miR-342–5p, mIR-494–5p, miR-501–3p, and mIR-629–3p were sharply downregulated, suggesting selective modulation of EMT and stress-related pathways. Importantly, the consistent downregulation of miR-3191–3p after CBD and IM mono treatments supports its use as a marker for chemotherapy response.

Further extending the IM-induced miRNA signature, several additional regulators with distinct functional implications were identified. miR-3615 was markedly upregulated (log2FC > 8.06). In gastric cancer, TOB1 drives production of exosomal hsa_circ_0008719, which binds and downregulates miR-3615 to promote autophagy

and suppress proliferation. By contrast, elevation of miR-3615 in our model may reflect a regulatory state that diverges from the TOB1–circRNA axis described in gastric tumors. miR-500a-3p was also induced. This miRNA is frequently reduced under injury and resistance states and has been reported to target MLKL, thereby alleviating necroptosis and attenuating inflammatory signalling in renal epithelial cells, consistent with a potential anti-inflammatory, cytoprotective role in K-562 cells. miR-885-5p upregulation aligns with previously described tumor-suppressive activities, including p53 stabilization and inhibition of migration and invasion. It has additionally been implicated in regulation of MMP9 in neuroinflammatory contexts, supporting a role in controlling inflammatory-associated matrix remodelling. Finally, a novel strand, hsa-miR-26-3p, was moderately elevated. Although members of the miR-26 family have been linked to Alzheimer's disease-related pathways and lung cancer biology, the functional significance of this novel 3p strand remains provisional and likely context dependent. Collectively, these observations indicate broad activation of tumor-suppressive and stress-responsive miRNAs in IM-sensitive cells, a pattern that contrasts with the widespread loss of such regulators observed in resistant phenotypes.

•CBD+IM elicit novel and synergistic miRNA responses

The combined treatment produced an exosomal miRNA signature dominated by pro-apoptotic and differentiation regulators. Among the most prominent changes was the strong upregulation of the master regulator of muscle differentiation, miR-1–3p (log2FC > 24), which has reported tumor-suppressive and pro-apoptotic activity, suggesting a profound shift in cell fate. In that particular treatment the tumor suppressor miR-133–3p, known to target BCL2 and inhibit growth, showed the highest level of induction, consistent with activation of potent apoptotic signalling. Additionally, the highly expressed hsa-miR311–5p and miR-33–3p suggests reprogramming of metabolic processes and possible activation of the AMPK pathway. Importantly, miR-4435, which is silenced in K-562R cells and further downregulated by CBD+IM treatment in K-562S cells, may reflect residual suppression of apoptotic networks in hematopoietic cells, despite its reported oncogenic role in solid tumors. Overall, CBD+IM induced a synergistic response in Imatinib-sensitive cells with marked amplification of apoptotic and differentiation signals, while partially retaining suppressive features.

Further extending the synergistic miRNA response, miR-122–3p was among the most highly upregulated species (log2FC > 25). miR-122 is a well-characterized tumor-suppressive miRNA with established roles in lipid metabolism and chemosensitivity in hepatocellular carcinoma; its pronounced induction here suggests activation of apoptotic and metabolic control pathways in IM-sensitive K562 cells. miR-311–5p was similarly robustly induced (log2FC > 24); although functional data for this strand are limited, its reproducible upregulation across replicates implies a potential role in stress adaptation or differentiation and therefore warrants targeted functional validation. Collectively, these changes support the notion that CBD+IM treatment amplifies apoptotic signalling while engaging metabolic and immune-related pathways in IM-sensitive cells, consistent with a multifaceted therapeutic response.

Comparative exosomal miRNA responses between K-562 R and K-562S across treatments

The applied treatments shaped a fundamentally divergent exosomal miRNA profiles in K-562R and K-562S cells, which is direct consequence of the sensitivity to the therapeutic regimen. CBD, IM, and CBD+IM each produced phenotype-specific miRNA signatures. Resistant cells consistently demonstrated loss of tumor-suppressive miRNAs and activation of stress-adaptive or oncogenic regulators, whereas sensitive cells predominantly responded through activation of apoptosis, differentiation, and metabolic related miRNAs.

CBD treatment

CBD modulated pro-apoptotic and differentiation related miRNAs in K-562S cells, evident by the marked upregulated miR-299–3p, miR-92b-5p, miR-34a-5p, and miR-1226–3p (Fig. 6A). In contrast, K-562R cells exhibited a dual response, involving simultaneous upregulation of tumor suppressors (miR-29b-3p, miR-29c-3p, miR-101–3p) and multiple oncogenic or inflammatory miRNAs (miR 21 3p, miR 362 3p/5p, miR 374a 5p). In resistant cells, CBD also triggered metabolic rewiring via miR-33a-5p and strong oxidative-stress signaling through miR-4463. A defining feature of the resistant phenotype was the persistent repression of miR-615–5p, which contrasted with its consistent activation by all treatments in K-562S cells, most prominently following CBD exposure alone.

IM treatment

In K-562S cells IM produced tumor-suppressive and stress-adaptive miRNA profile encompassing the robustly induced miR-133a-3p, miR-3173–5p, miR-500a-3p, miR-548e-3p, and miR-885–5p (Fig. 6B). However, in K-562R cells, IM caused widespread loss of tumor-suppressive and regulatory miRNAs (miR-429, miR-532–3p, miR-1284, miR-760, miR-9–5p and the underexplored let-7g-3p). Additionally, stress-tolerance related miRNAs, such as miR-1226–5p, miR-3619–3p, and miR-3667–5p were upregulated in resistant cells. The most pronounced contrast was miR-3191-3p, which was strongly upregulated in K-562 R but sharply downregulated in K-562S, marking it as a robust resistance-associated discriminator.

CBD+IM combination treatment

The combined treatment strongly induced miR-1–3p, miR-133–3p, miR-122–3p, miR-311–5p, and miR-33–3p which are related to apoptotic and differentiation pathways in K-562S cells (Fig. 6C). Conversely, in K-562R cells CBD+IM only partially restored the apoptotic signaling, primarily through miR-204–3p, miR-107, miR-138–5p, and miR-3689b-5p. Tumor-suppressive or regulatory miRNAs (let-7g-3p, miR-153–3p, miR-615–3p/5p) remained deeply suppressed in resistant cells along with continued repression of immmune- and metabolism-related miRNAs (miR-1304–5p, miR-181–5p, miR-3176, miR-1273h-5p). miR-3121-3p, reported to have oncogenic associations, remained strongly downregulated only in resistant cells, indicating persistent dysregulation of survival pathways.

GO enrichment analysis—biological processes

To investigate the biological roles of exosomal miRNA`s target genes in Imatinib-resistant (K562-R) and Imatinib-sensitive (K562-S) cells, a GO biological process enrichment analysis was performed after exposure to CBD, IM, and their combination (CBD+IM). Significantly enriched GO terms (adjusted p-value(Q) < 0.05) were grouped into two categories: common enriched processes in all treatments and those specific to an individual treatment condition. The enrichment ratios for each term were used to assess the relevance of the overrepresented targets of differentially expressed miRNAs.

In the present study, we employed an inductive approach, beginning with common GO terms and progressing toward treatment-specific pathways, as presented below. The detailed results of the Gene Ontology (GO) enrichment analysis for K-562R cells (Fig. 7 a, b, c) and K-562S cells (Fig. 8 a, b, c) (IM, CBD, and COMBO treatments) are provided in Supplementary Tables S7–S12.

•Functional analysis of exosomal miRNA target genes in Imatinib-resistant K562-R cells following drug treatment

Common biological processes between treatments

Regardless of the applied treatment, GO enrichment analysis of the exosomal miRNA-target genes in Imatinib-resistant K-562R cells identified distinct consistently overrepresented biological processes. These were predominantly related to three functional groups: Transcriptional Regulation, Development and Morphogenesis, and Phosphorylation and Post-Translational Regulation. The most

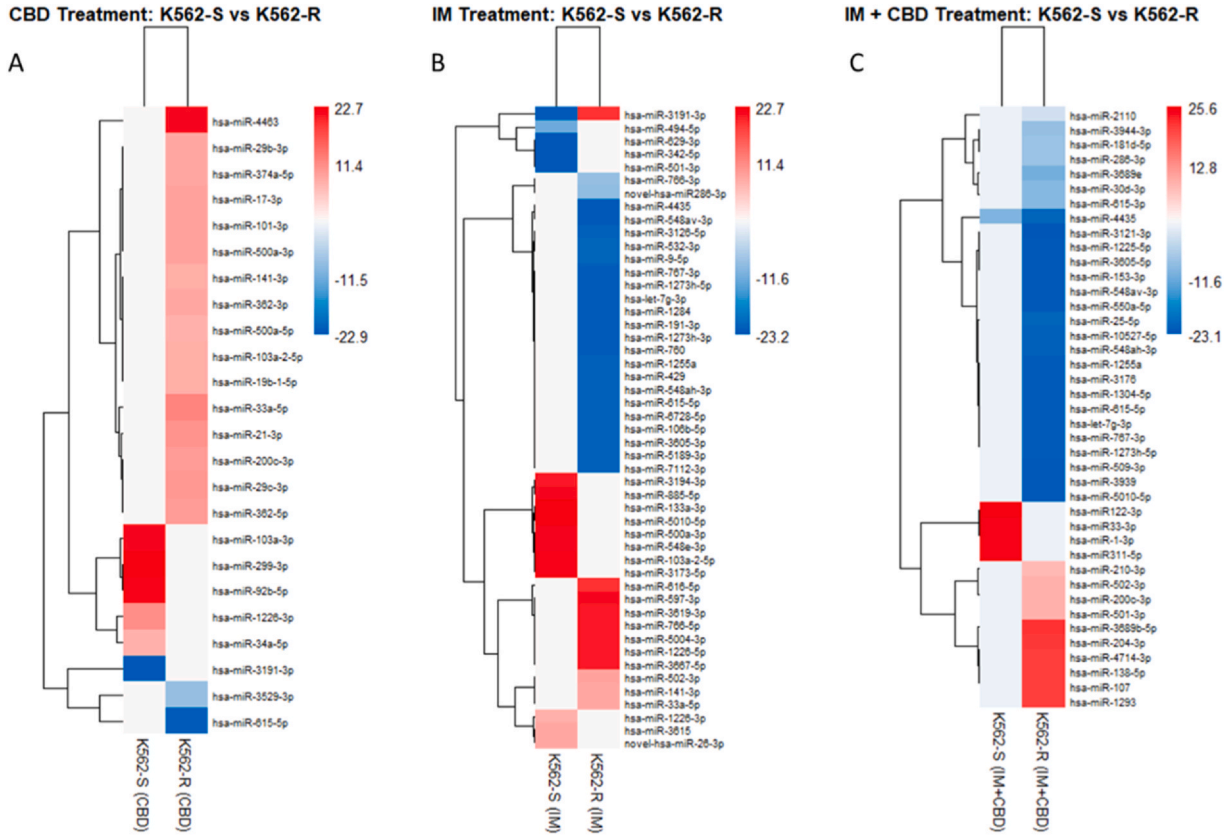

Fig. 6. Differential exosomal miRNA expression between Imatinib-sensitive (K-562S) and Imatinib-resistant (K-562 R) cells across treatments. Differentially expressed exosomal miRNAs between K-562S and K-562 R cells following 48 h treatment with cannabidiol (CBD), Imatinib mesylate (IM), or their combination (CMB = CBD+IM). Complete lists of differentially expressed miRNAs, including treatment-specific signatures, are provided in Supplementary Tables S1–S6. (a) Heatmap showing differential miRNA expression between K-562S and K-562 R cells under CBD treatment. Expression values are presented as log2 fold change (log2FC) with Benjamini–Hochberg-adjusted p ≤ 0.05. (b) Heatmap showing differential miRNA expression between K-562S and K-562 R cells under IM treatment. Expression values are presented as log2FC with Benjamini–Hochberg-adjusted p ≤ 0.05. (c) Heatmap showing differential miRNA expression between K-562S and K-562 R cells under combined (CBD+IM) treatment. Expression values are presented as log2FC with Benjamini–Hochberg-adjusted p ≤ 0.05. Color scales indicate relative up- or down-regulation of miRNAs, highlighting treatment-dependent differences between the sensitive and resistant phenotypes.

enriched term, i.e., part of the transcriptional cluster, was positive regulation of transcription by polymerase II (GO:0045944; CBD: 0.838, IM: 0.978, CBD + IM: 0.976). Nervous system development (GO:0007399; CBD 0.885, IM 0.991, CBD + IM 0.993) in Development and Morphogenesis and phosphorylation (GO:0016310; CBD 0.847, IM 0.986, CBD + IM 0.980) in Phosphorylation and Post-Translational Modification were also highly enriched.

GO terms shared by at least two treatments (pairwise overlaps)

Several additional processes showed a high level of enrichment shared by at least two treatment conditions, revealing substantial but, at the same time, non-universal overlap. For example, intracellular signal transduction (GO:0035556—CBD: 0.840; IM: 0.992) formed a Signal Transduction cluster, which was a common hub between CBD and IM, likely due to activation of the conserved cascade. The Phosphorylation and Post-Translational Modification and Enzyme Activation Regulation

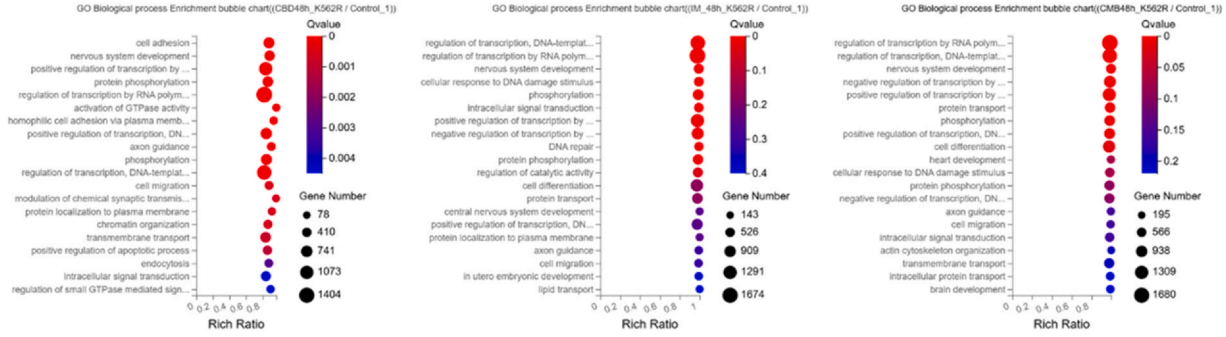

Fig. 7. Gene Ontology (GO) enrichment analysis of exosomal miRNA target genes in K-562R cells following 48 h treatment. (a) Bubble plot of GO enrichment for target genes of differentially expressed exosomal miRNAs after cannabidiol (CBD) exposure, showing the top 20 biological processes ranked by adjusted p values (Q ≤ 0.05, Benjamini–Hochberg correction). (b) Bubble plot of GO enrichment for target genes of differentially expressed exosomal miRNAs after Imatinib mesylate (IM) exposure, showing the top 20 biological processes ranked by adjusted p values (Q ≤ 0.05). (c) Bubble plot of GO enrichment for target genes of differentially expressed exosomal miRNAs after combined CBD+IM treatment (COMBO), showing the top 20 biological processes ranked by adjusted p values (Q ≤ 0.05). Bubble size represents the number of target genes annotated to each GO term, bubble color indicates enrichment significance (redder = lower Q value), and the x axis depicts the enrichment ratio (candidate gene number/term gene number).

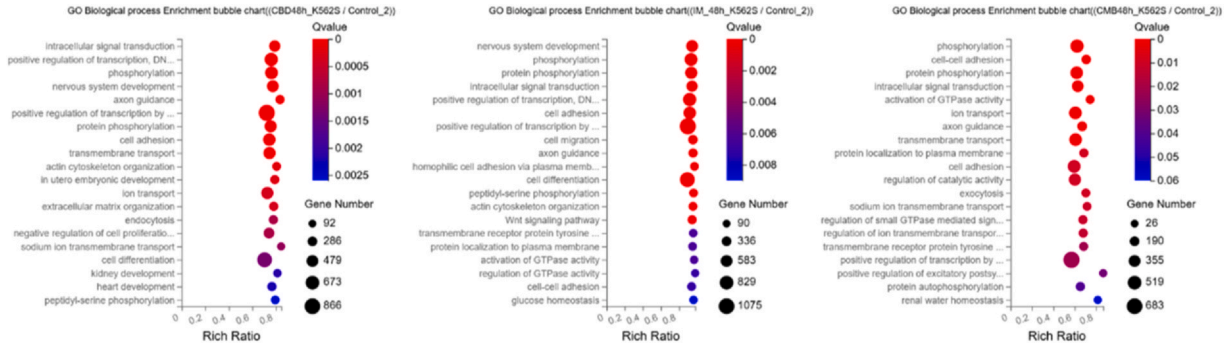

Fig. 8. Gene Ontology (GO) enrichment analysis of exosomal miRNA target genes in K-562S cells following 48 h treatment. (a) Bubble plot of GO enrichment for target genes of differentially expressed exosomal miRNAs after cannabidiol (CBD) exposure, showing the top 20 biological processes ranked by adjusted p values (Q ≤ 0.05, Benjamini–Hochberg correction). (b) Bubble plot of GO enrichment for target genes of differentially expressed exosomal miRNAs after Imatinib mesylate (IM) exposure, showing the top 20 biological processes ranked by adjusted p values (Q ≤ 0.05). (c) Bubble plot of GO enrichment for target genes of differentially expressed exosomal miRNAs after combined CBD+IM treatment (COMBO), showing the top 20 biological processes ranked by adjusted p values (Q ≤ 0.05). Bubble size represents the number of target genes annotated to each GO term, bubble color indicates enrichment significance (redder = lower Q value), and the x axis depicts the enrichment ratio (candidate gene number/term gene number).

hubs were expanded in the CBD-IM intersection with protein phosphorylation (GO:0006468—CBD: 0.863; IM: 0.984) and regulation of catalytic activity (GO:0050790—CBD: 0.826; IM: 0.983), respectively. These pairwise-shared processes show a core regulatory framework maintained between all treatments, while certain signalling and enzymatic control elements are preferentially activated under specific drug treatments.

CBD-specific enrichment

In terms of experimental arm specifics, characteristic signatures were observed. The exposure to CBD produced a broad enrichment profile encompassing several hubs, including Adhesion and Extracellular Interactions (e.g. homophilic cell adhesion via plasma membrane adhesion molecules (GO:0007156; RR: 0.93)); Migration, Motility and Angiogenesis (e.g. negative chemotaxis (GO:0050919; 1.00)); and Signal Transduction (activation of GTPase activity (GO:0090630; 0.97)). Maximal enrichment was found for establishment of cell polarity (GO:0030010; 1.00) under the Cytoskeleton and Structural Organization functional group. Additionally, CBD-profiled miRNA-target genes enriched terms in the following functional groups: Ion Transport and Homeostasis (transmembrane transport-related terms (GO:0055085, 0.84; GO:0035725, 0.92)); Phosphorylation and Post-Translational Modifications (protein phosphorylation processes (GO:0018108, 0.89; GO:0046777, 0.87)); Vesicle Trafficking and Membrane Transport (vesicle-mediated membrane trafficking

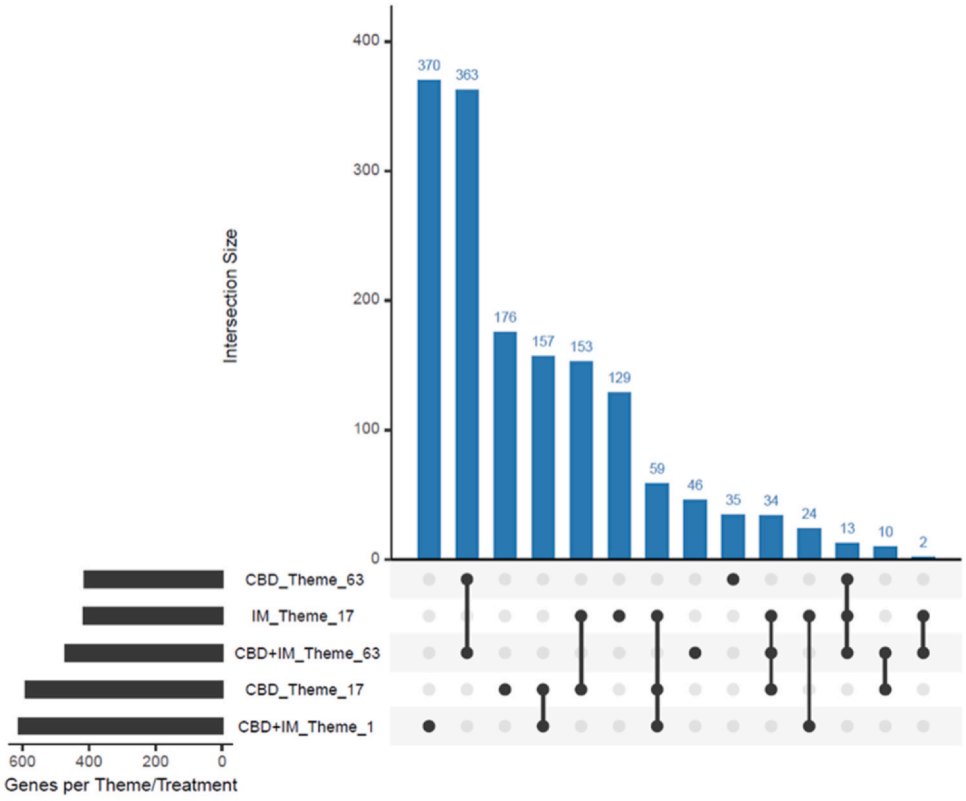

Fig. 9. UpSet plot of interconnected biological themes in K-562R cells across all treatments. CBD-related Themes. Subnetworks uniquely associated with CBD treatment were those regulating vesicle trafficking and endocytosis (Theme 20) (e.g., multivesicular body sorting, lysosomal transport, clathrin-mediated uptake), together with stress/survival signalling (Theme 19) (p53, MAPK/ERK, NF-kB, PI3K/AKT, TOR). Alongside these, other recurring themes were ribosome biogenesis, transcriptional regulation, and immune signalling. Overall, CBD-responsive miRNAs appear to modulate genes involved in intracellular transport, stress adaptation, and paracrine communication, in addition to sustained core biosynthetic functions.

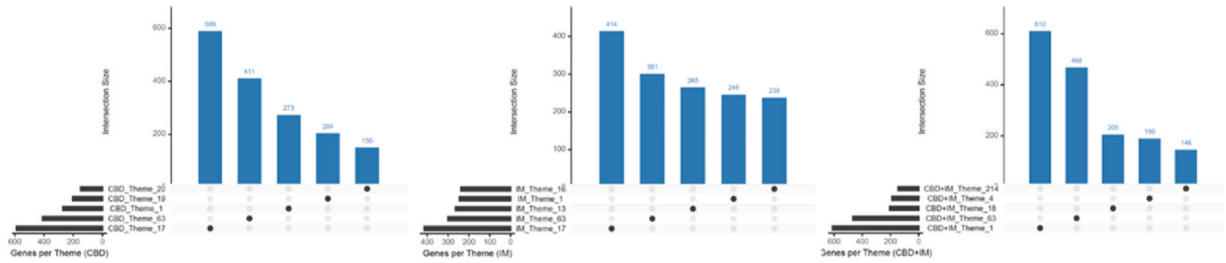

Fig. 10. UpSet plots of treatment specific biological themes in K-562R cells. (a) CBD related subnetworks enriched in vesicle trafficking/endocytosis and stress/survival signalling, alongside recurring ribosome and transcriptional modules. (b) IM related subnetworks enriched in nucleotide catabolism and DNA repair/meiotic recombination, integrated with biosynthetic and immune themes. (c) CBD+IM related subnetworks enriched in mitochondrial outer membrane permeabilization (MOMP), apoptosis regulation, and developmental/regenerative programs, integrated with ribosome, transcriptional, and immune signalling.

(GO:0072659, 0.91; GO:0006897, 0.88)); and Transcriptional Regulation (chromatin organization (GO:0006325; 0.86)). Hubs such as Stress and Cell Fate (positive regulation of apoptotic process (GO:0043065; 0.86) and negative regulation of cell proliferation (GO:0008285; 0.84)), together with Development and Morphogenesis (axon guidance (GO:0007411), heart looping (GO:0001947), in utero embryonic development (GO:0001701)), and Neural and Synaptic Signalling (synapse-related processes (GO:0050808; GO:0050804; GO:0048167)) also showed a high enrichment ratio.

IM -specific enrichment

In contrast, mono treatment with IM produced centered enrichment within the Stress and Cell Fate functional group, revealing activated genotoxic stress and repair mechanisms through cellular response to DNA damage stimulus (GO:0006974; 0.99) and DNA repair (GO:0006281; 0.99) terms. These processes were not observed in CBD-specific or CBD+IM-specific networks, which reveals a possible IM-driven DNA surveillance program in Imatinib-resistant cells.

CBD+IM-specific enrichment

Following the combined treatment, dominant treatment-specific GO terms were part of the Development and Morphogenesis (cell differentiation (GO:0030154; 0.97)) and Vesicle Trafficking and Membrane Transport groups (protein transport (GO:0015031; 0.98)). This reveals a cooperative effect between CBD and IM in lineage-related transcriptional programs.

Overall, while the three treatment conditions shared functionally enriched pathways in transcriptional regulation and phosphorylation, CBD uniquely modeled adhesion, polarity, motility, and neuromorphogenetic pathways; IM alone triggered DNA damage response and repair; and CBD+IM combination elevated differentiation and protein transport capacity. Together, these partially overlapping networks reflect a nuanced exosomal miRNA-mediated regulation in the context of IM resistance.

•Functional analysis of exosomal miRNA target genes in Imatinib-sensitive K562-S cells following drug treatment

Common biological processes between treatments

Throughout all three treatments in K-562S cells a consistently enriched set of GO terms was uncovered, extending over Signal Transduction, Phosphorylation and Post Translational Modification, Transcriptional Regulation, Adhesion and Extracellular Interactions, Ion Transport and Homeostasis, Development and Morphogenesis,

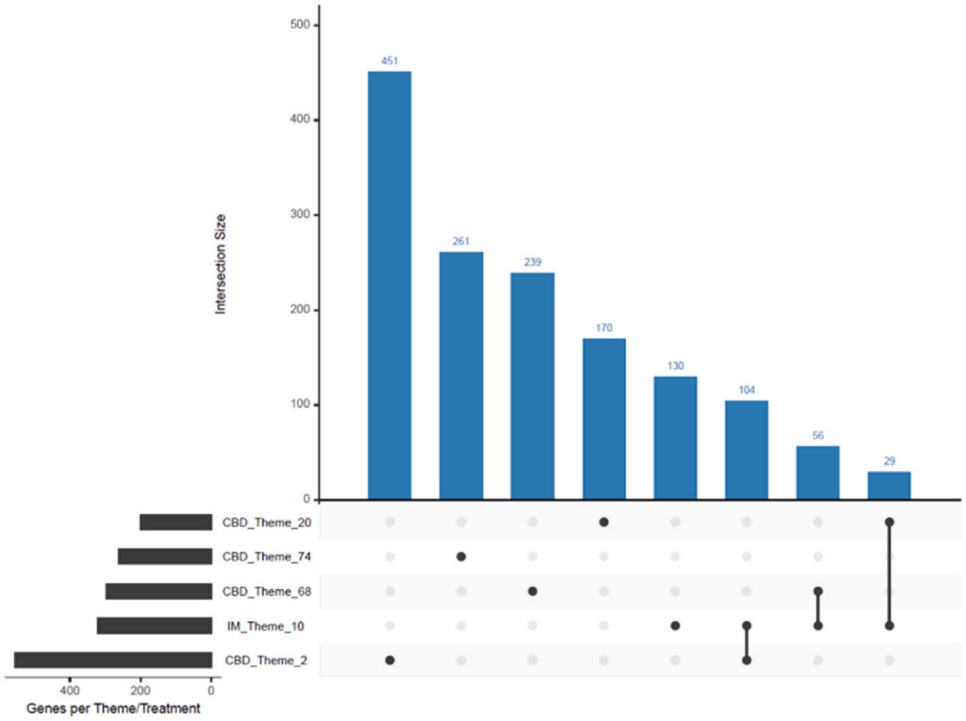

Fig. 11. UpSet plot showing interconnected biological themes in K-562S cells across treatments. UpSet analysis of exosomal miRNA target gene subnetworks in Imatinib sensitive (K-562S) cells following 48 h exposure to cannabidiol (CBD), Imatinib mesylate (IM), or their combination (CBD+IM). The plot depicts overlapping and unique biological themes enriched across treatments, highlighting cross connected modules of transcriptional regulation, DNA repair, glial/neural differentiation, and immune signalling. Bar height indicates the number of genes associated with each theme, while connected dots represent intersections between functional modules.

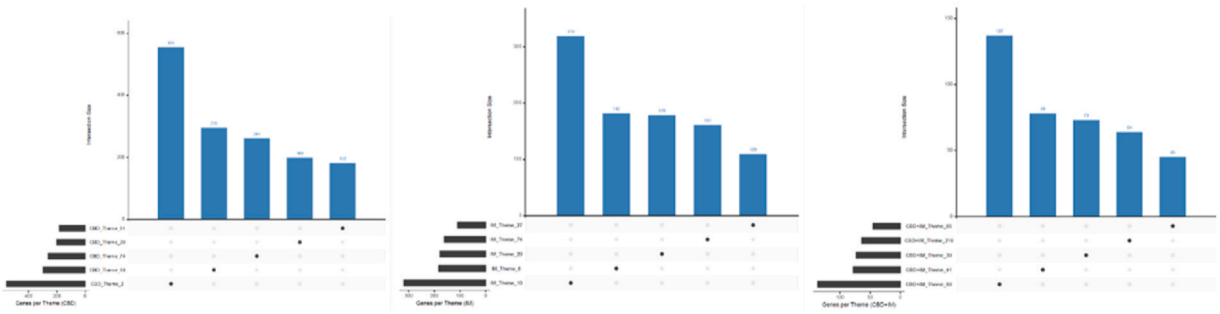

Fig. 12. UpSet plots of treatment specific biological themes in K-562S cells. (a) CBD related subnetworks enriched in lipid and sphingolipid metabolism, alongside recurring transcriptional, ribosomal, DNA repair, and immune modules. (b) IM related subnetworks enriched in RNA metabolism/processing and developmental/regenerative programs, integrated with glial/neural differentiation and biosynthetic modules. (c) CBD+IM related subnetworks enriched in microtubule-based transport, cell cycle checkpoint control, mitotic spindle organization, cardiovascular development, and DNA repair, integrated with recurring transcriptional and genome maintenance themes.

and Enzyme Activity Regulation. Within Signal Transduction the most enriched term was intracellular signal transduction (GO:0035556), while protein autophosphorylation was the top overrepresented process (GO:0046777) under Phosphorylation and Post Translational Modification. Single representative terms fell under Transcriptional Regulation (positive regulation of transcription by RNA polymerase II (GO:0045944)), Adhesion and Extracellular Interactions (cell adhesion (GO:0007155)), Development and Morphogenesis (axon guidance (GO:0007411)), and Enzyme Activity Regulation (regulation of catalytic activity (GO:0050790)). The ion Transport and Homeostasis functional group included transmembrane transport processes (GO:0055085; GO:0035725).

Additionally, evidence of treatment-contingent reinforcements was the large number of shared processes between two treatments. For example, single GO terms were found to be enriched in many shared functional groups, particularly for Transcriptional Regulation (positive regulation of transcription, DNA-templated (GO:0045893)[CBD;IM]), Phosphorylation and Post Translational Modification (peptidyl-serine phosphorylation (GO:0018105)[CBD;IM]), Neural and Synaptic Signalling (modulation of chemical synaptic transmission (GO:0050804)[CBD;IM]), Ion Transport and Homeostasis (calcium ion transmembrane transport (GO:0070588)[CBD;IM]), and Cytoskeleton and Structural Organization (actin cytoskeleton organization (GO:0030036)[CBD;IM]). The largest hub, Development and Morphogenesis, contained five common terms, with negative regulation of neuron projection development (GO:0010977[CBD;IM]). Additional overlaps under Migration, Motility and Angiogenesis group were the jointly between IM and CBD enriched angiogenesis (GO:0001525) and cell migration (GO:0016477) terms. Finally, Ion Transport and Homeostasis formed a shared hub between CBD and CBD+IM, encompassing two important ion transport-related GO terms (GO:0034765; GO:0006811). Collectively, these patterns reveal a stable miRNA-regulated core network complemented by treatment-dependent variations in signalling, structural, ion transfer and developmental processes.

CBD-specific enrichment

The CBD specific enrichment of exosomal miRNA-target genes broad to light a range of cellular processes represented by ten major functional domains. CBD exerted potential activation of cell–matrix remodeling effects by enriching terms within Adhesion and Extracellular Interactions (GO:0030198, RR:0.78; GO:0051893, RR:0.96) hub. The activated synapse assembly (GO:00074165, RR:0.87) under Neural and Synaptic Signalling hub demonstrated

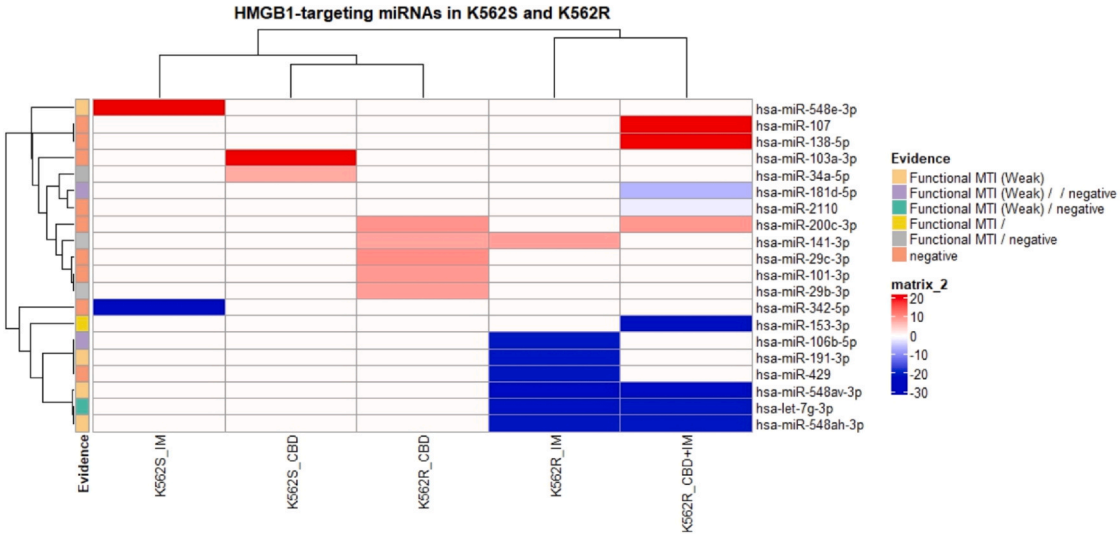

Fig. 13. Heatmap showing differential expression of 20 miRNAs previously evaluated for HMGB1 targeting across K562S and K562R cells treated with CBD, IM, or CBD+IM. Rows represent individual miRNAs and columns represent treatment conditions. Colors indicate log2 fold-change values relative to untreated controls. Row annotations denote the type of experimental evidence available for each miRNA–HMGB1 interaction, as retrieved from multiMiR. Most miRNAs were classified as negative, indicating no confirmed interaction in prior studies, while a subset carried Functional MTI or Functional MTI (Weak) labels, reflecting low-confidence or context-dependent functional support. These evidence categories are displayed in the accompanying legend. Hierarchical clustering highlights distinct expression patterns separating K562S and K562R phenotypes, with several miR-548 family members and miR-153-3p showing pronounced treatment-specific regulation.

CBD-responsive miRNAs could be linked to neural plasticity. Further, the overrepresented terms in Cytoskeleton and Structural Organization (GO:0007010, RR:0.78; GO:0030010, RR:0.91) demonstrate potential effect on cell shape and migration directionality, while the terms found under Development and Morphogenesis highlight CBD` impact on differentiation and tissue-patterning pathways (GO:0001822, RR:0.81; GO:0031175, RR:0.80; GO:0007528, RR:0.92). Ion Transport and Homeostasis was represented by terms regulating fluid balance and excitability (GO:0003091, RR:0.92; GO:0071805, RR:0.78; GO:0006813, RR:0.78). Both, negative and the positive regulation of cell migration (GO:0030336, RR:0.80; GO:0030335, RR:0.75) exerted high rich ratio under Migration, Motility and Angiogenesis. Additional single terms were found to be distributed over several hubs, including peptidyl-tyrosine phosphorylation (GO:0018108, RR:0.78) in Phosphorylation and Post-translational Modification, canonical Wnt signalling pathway (GO:0060070, RR:0.86) in Signal Transduction, negative regulation of cell proliferation (GO:0008285, RR:0.74) in Stress and Cell Fate, and endocytosis (GO:0006897, RR:0.78) in Vesicle Trafficking and Membrane Transport. Together these findings suggests that CBD shapes broad miRNA-mediated regulatory networks, potentially modulating both neural and peripheral cellular functions via coordinated control of adhesion, signalling, structural dynamics, and homeostasis.

IM-specific enrichment

The IM-specific enrichment was more focused. Terms, relevant to leukemic cell clustering and communication formed Adhesion and Extracellular Interactions (GO:0007156, RR:0.97)(GO:0007229, RR:0.95) indicating probable modulation of direct cell–cell contacts. The enrichment of glucose homeostasis (GO:0042593, RR:0.96) under Endocrine and Metabolic Regulation confirm IM`s known potential to rewire leukemia cell metabolism via exosomal communication. Additional terms were found within Signal Transduction (GO:0043087, RR:0.98; GO:0007264, RR:0.94) suggesting modulation of cytoskeletal dynamics and intercellular signalling. Within Stress and Cell Fate, enrichment of negative regulation of neuron apoptotic process (GO:0043524, RR:0.94) reflects a shift toward anti-apoptotic processes, while response to hypoxia (GO:0001666, RR:0.93) indicates activation of adaptive response to low-oxygen niches and activation of early resistance mechanisms.

CBD+IM combination-specific enrichment

The combined treatment (CBD+IM) produced a distinct enrichment profile. Terms in Neural and Synaptic Signalling (positive regulation of excitatory postsynaptic potential (GO:2000463; 0.87) and Vesicle Trafficking and Membrane Transport (exocytosis (GO:0006887; 0.70) were specifically overrepresented hinting at coordinated activation of membrane trafficking and synapse-related signalling possibly revealing additive or synergistic drug effects on intercellular communication pathways.

PPI-MCODE analysis

K-562R: Cross-connected Themes

In the resistant K-562R cell line, the UpSet analysis revealed three major interconnected biological themes: ribosome biogenesis (Theme 63), global transcriptional regulation (Theme 17), and immune/inflammatory signalling (Theme 1) (Fig. 9). These modules were found to be functionally coupled, with ribosome production (Theme 63) overlapping with transcriptional regulation (Theme 17), and transcription programs (Theme 17) intersecting with cytokine signalling (Theme 1), particularly under CBD+IM. Taken together, these indicate that resistant cells maintain a coordinated biosynthetic and immune network as part of an integrated stress-adaptive program.

K-562R: CBD-related Themes

Uniquely associated with CBD treatment subnetworks were those regulating vesicle trafficking and endocytosis (Theme 20) (e.g., multivesicular body sorting, lysosomal transport, clathrin-mediated uptake), together with stress/survival signalling (Theme 19) (p53, MAPK/ERK, NF-kB, PI3K/AKT, TOR). Alongside these, recurring were also themes related to ribosome biogenesis, transcriptional regulation, and immune signalling. Overall, CBD-responsive miRNAs appear to modulate genes involved in intracellular transport, tress adaptation, and paracrine communication, in addition to sustained core biosynthetic functions (Fig. 10A).

K-562R: IM-related Themes

The exposure to IM revealed miRNA-target genes that enriched subnetworks related to nucleotide catabolism and metabolic adaptation (Theme 16) and DNA repair/meiotic recombination processes (Theme 13) (chromatid cohesion, homologous recombination, double-strand break repair). These functional groups were paralleled by recurring biosynthetic and immune modules. Thus, the exosomal miRNAs profiled by IM treatment in resistant cells might be linked to regulation of genome maintenance and metabolic turnover, while maintaining ribosomal and transcriptional activity (Fig. 10B).

K-562R: CBD+IM-related Themes

The concomitant application of CBD and IM created a distinct profile of subnetworks related to mitochondrial outer membrane permeabilization (MOMP) and apoptosis regulation (Theme 214), as well as developmental/regenerative programs (Theme 4)(endocrine, hepatic, mammary, skin, and neural pathways), and glial/neural differentiation (Theme 18) (gliogenesis, myelination, blood–brain barrier formation). Similarly to the mono treatments, these unique modules were integrated with recurring ribosome, transcriptional, and immune signalling themes. Collectively, miRNAs modulated by the combination of CBD+IM are indicative of a complex adaptive landscape that combines apoptotic checkpoints and developmental programs with biosynthetic and inflammatory regulation (Fig. 10C).

K-562S: Cross-connected Themes

Several large interconnected biological themes were identified in IM-sensitive K-562S cells: transcriptional regulation (Theme 20), DNA repair (Theme 68), and glial/neural differentiation (Theme 10), with immune signalling also integrated into this network (Theme 2) (Fig. 11). In K-562S cells, glial/neural differentiation emerged as a central hub, cross-connected with transcriptional and DNA repair subnetworks that were further linked to immune signalling. By contrast, the ribosome biogenesis hub of the GO terms (CBD, Theme 74) appeared to be a module restricted to the CBD treatment alone, which causes it to be more isolated from the main gene cluster. Overall, the observed architecture of the miRNA-mediated network highlights a noticeable adaptive program in K-562S cells, in contrast to the ribosome/transcription/immune gene regulation framework observed in K-562R cells.

K-562S: CBD-related Themes

The treatment with CBD led to enrichment of miRNA-target genes part of unique subnetworks related to lipid and sphingolipid metabolisms (Theme 61), revealing potential regulation of membrane remodeling and bioactive lipid pathways. An indication for CBD-profiled miRNA response that could orchestrate metabolic and biosynthetic programs in K-562S cells were the coinciding recurring modules of transcriptional control (Theme 20), ribosome biogenesis (Theme 74), DNA repair (Theme 68), and immune signalling (Theme 2) (Fig. 12A).

K-562S: IM-related Themes

The application of IM leads to enrichment of mIRNA-regulated gene subnetworks such as RNA metabolism and processing (Theme 27), including 3′-end processing and miRNA maturation, indicating broad interactions in RNA metabolism. In addition, IM-profiled miRNAs possess the specificity to interact with gene hubs that are part of developmental and regenerative programs (Theme 6) encompassing multiple tissues, along with glial/neural differentiation processes (Theme 10). All of these functional clusters were integrated with recurring biosynthetic (Theme 74) and transcriptional

modules (Theme 20), showing that IM-responsive miRNAs in K-562S cells could coordinate RNA processing together with lineage-related and developmental pathways (Fig. 12B).

K-562S: CBD+IM-related Themes

The combined treatment revealed characteristic subnetworks associated with microtubule-based transport and organelle trafficking (Theme 65), cell cycle checkpoint control (Theme 218), and mitotic spindle/centrosome organization (Theme 39), along with cardiovascular developmental programs (Theme 41). DNA repair pathways were also observed, consistent with the recurring genome maintenance Theme 68. Collectively, CBD+IM-responsive miRNAs in IM-sensitive K562 cells appear to regulate intracellular transport, mitotic architecture, developmental morphogenesis, and DNA repair, reflecting a multifaceted adaptive response that integrates cell cycle regulation, genome stability, and organelle dynamics (Fig. 12C).

Exosomal HMGB1 targeting miRNA profiles

The differential expression analysis of K-562S and K-562R cells exposed to CBD, IM, or their combination brough to light 20 previously evaluated HMGB1 targeting miRNAs (Fig. 13). Annotations retrieved from multiMiR provide evidence that most miRNAs in this dataset were classified as negative, suggesting that prior studies did not confirm direct HMGB1-miRNA interactions. However, a subset of miNRAs displayed Functional MTI or Functional MTI (Weak) annotations, implying low-confidence or context-dependent functional effects. Among these, miR-153–3p is distinguished with strongest support, marked by clear Functional MTI label. Additional candidates with weak functional evidence were miR-191–3p, miR-548av-3p, miR-548ah-3p, and miR-548e-3p, two of which exhibited some of the largest treatment-associated fold changes. These miRNAs form distinct expression clusters that separate K-562S from K-562R phenotypes, with K-562R cells showing pronounced downregulation of miR-153–3p and multiple miR-548 family members under IM and CBD+IM treatments. Taken together, these findings delineate a small set of miRNAs that show strong differential expression and at least weak functional evidence, positioning them as candidates for further investigation into HMGB1-related regulatory mechanisms.

Discussion

CI and DRI of combined treatment

The combination of CBD and IM produced characteristic responses in sensitive versus resistant K562 cells. In K-562S cells, a dose-dependent synergy was discovered. While certain low-dose combinations elicited antagonism, treatments with clinically relevant concentrations elicited strong synergy. These heterogenic effects demonstrate that, in sensitive cells, the balance between pleiotropic effects of CBD and targeted inhibition of IM can vary depending on dose ratios, emphasizing the need for careful dose titration in order to avoid antagonism. At synergistic concentrations, CBD contributed to substantial dose reduction, revealing potential for lowering IM dose and reducing drug burden while also preserving efficacy.

In K-562R cells, the combined treatment induced a uniform and consistently synergistic response. Dose reduction indices for IM were significantly elevated in comparison to sensitive cells, accompanied by sustained CI values within the synergistic range. This pattern reveals chemo-sensitization to IM induced by CBD in resistant cells, likely mediated through modulation of survival signalling and disruption of adaptive resistance mechanisms. Notably, CBD's capacity to simultaneously lower the required IM dose while enhancing its efficacy presents a dual therapeutic advantage: restoration of drug sensitivity and reduction in treatment-related toxicity.

Taken together, these findings support the hypothesis that co-administration of CBD may expand IM`s therapeutic window. The important difference is that while in K-562S cells CBD contribute to dose optimization, in K-562R cells the synergistic effect with IM may lead to direct mitigation of resistance. Such a complementary effects highlight the potential of CBD as an adjunct to the treatment protocol of leukemia, although further mechanistic and translational studies are necessary.

Differential miRNA profile of K-562R and K-562S derived vesicles

The comparative analysis of exosomal miRNAs released by K-562R and K-562S cells following exposure to CBD, IM, and CBD+IM revealed distinctive regulatory architecture reflecting sensitivity or resistance traits of each phenotype. In resistant cells the various treatments elicited loss of canonical tumor suppressors, enrichment of stress adaptive and metabolic regulators and induced poorly annotated miRNAs that may be important to the microenvironmental conditioning. In contrast, the sensitive cells responded to the treatments with consistent activation of apoptotic, differentiation related, and tumor-suppressive miRNAs, which is an indication of preserved responsiveness to the applied therapeutic intervention. Together, these findings demonstrate the exosomal miRNAs` potential as reporters of treatment response and mediators of resistance.

CBD treatment: tumor-suppressive response in K-562S versus dual signalling in K-562R

The strong induction of miR-299–3p [29], miR-92b-5p [30], miR-34a-5p, miR-103a-3p, and miR-1226–3p by CBD in K-562S cells reveals predominant engagement of pro-apoptotic and tumor suppressive responses. These miRNAs are linked to BCL2 inhibition, metabolic stress, and differentiation, suggesting that CBD reinforces intrinsic apoptotic pathways in the IM sensitive phenotype. Conversely, dual and conflicting regulatory programs were triggered by CBD in K-562R cells. While several tumor suppressors (miR-29b-3p, miR-29c-3p, miR-101–3p) were induced, resistant cells simultaneously upregulated oncogenic and inflammatory miRNAs, including miR-21–3p [31], mIR-362–3p/5p [32], miR-17–3p, miR-19b-1–5p, and miR-374a-5p. These miRNAs are implicated in PI3K/AKT, NK-kB, and STAT3 signalling, suggesting that resistant cells mobilize compensatory survival pathways that mitigate the CBD-induced stress. Further, the induction of miR-33a-5p [33] and miR-200 family members signifies for rewiring of metabolic and stromal interactions. In the same time the sharp repression of miR-615–5p is consistent with persistent suppression of apoptotic control. Overall, in sensitive cells, CBD promotes a unidirectional pro-apoptotic response, whereas in resistant cells it triggers the simultaneous activation of suppressive and oncogenic miRNA networks, reflecting a stress-buffering phenotype characteristic of IM resistance.

IM treatment: restoration of suppressive signalling in K-562S versus widespread suppressor loss in K-562R

IM treatment in K-562S cells evoked broad activation of tumor-suppressive and stress-responsive miRNAs, including miR-133a-3p [34], miR-5010–5p [35], miR-548e-3p, miR-500a-3p, miR-885–5p, and miR-1226–3p. These miRNAs are involved in apoptosis regulation, necroptosis attenuation, metabolic control, and inflammatory signalling, which is in alignment with IM`s expected pro-apoptotic and anti-proliferative effects in the sensitive phenotype. Furthermore, the induction of miR-3615 and miR-26–3p suggests involvement of autophagy and chromatin-associated pathways. However, the induction of oncogenic miR-3173–5p [36], reported with context-dependent roles in cancer progression, demonstrates a complex response to IM in sensitive cells.

In an opposing pattern, IM exposure in K-562R cells resulted in stress adaptive but suppressor deficient miRNA landscape. Despite the upregulation of miR-1226–5p [37] and miR-3191–3p [38], which are both linked to stress tolerance and radioresistance, the dominant

response was strong repression of miRNAs with tumor-suppressive or context-dependent roles, including miR-429 [39], miR-532–3p, miR-1284, miR-760, miR-9–5p, miR-767–3p, several miR-548 [40] family members, and the less-characterized let-7g-3p [41]. Further, an indication for loss of apoptotic, metabolic and extracellular signalling control was demonstrated by the downregulated of miR-615–5p, miR-5189–3p, miR-6728–5p, miR-7112–3p, and miR-3605–3p. Moreover, the pronounced repression of miR-3126–5p and miR-286–3p, which are both predicted to interact with chromatin regulators and JNK associated pathways, points to treatment-induced alterations in epigenetic and stress-response regulation. Collectively, IM reinforces tumor-suppressive signalling in sensitive cells, but in resistant cells it amplifies suppressor loss and may promote a more robust resistant phenotype alongside survival-oriented exosomal communication.

CBD+IM treatment: synergistic amplification in K-562S versus partial restoration in K-562R

The combined treatment in K-562S cells produced synergistic activation of apoptotic and differentiation associated miRNAs. The exposure to CBD+IM massively induced miR-1–3p [42], miR-133a-3p [43], miR-122–3p, miR-311–5p, and miR-33–3p [44] which testifies for coordinated activation of apoptosis, lineage commitment, and metabolic reprogramming. This profile suggests that CBD may enhance IM mediated cytotoxicity by amplification of miRNA driven pathways related to apoptosis and differentiation. On top of that the persistant suppression of miR-4435, despite its oncogenic role in solid tumors [45], might be considered as a context dependent regulatory function in hematopoietic cells, possibly reflecting attenuated stromal interaction signalling rather than classical tumor suppression.

In comparison, exposure of K-562R cells to CBD+IM led to partial reactivation of apoptotic control, primarily evident by the induction of miR-204–3p, miR-1226–3p [46,47], and stress adaptive regulators such as miR-107, miR-138–5p, and miR-3689b-5p [48–50]. However, the combination failed to restore key tumor-suppressive miRNAs, as well as the underexplored let-7g-3p, miR-153–3p [51], and both strands of miR-615. Further, the persistent repression of miR-4435, miR-1304–5p, miR-181d-5p, miR-3176, miR-1273h-5p, and miR-5010–5p provides evidence for treatment-induced continued impairment of immune regulation, metabolic adaptation, and anti-inflammatory signalling. Importantly, despite the observed partial apoptotic restoration the sustained dysregulation of oncogenic miR-3121–3p [52] in parallel with the repression of miR-25–5p, miR-30d, miR-3605–5p, and miR-3689e suggests that resistant cells continue to maintain a residual oncogenic and stress tolerant exosomal signalling. Thus, while in sensitive cells CBD+IM elicited synergistic cytotoxic effect, in resistant cells that combination yields only incomplete reversal of suppressor loss, indicating that the combined therapy can only mitigate but not fully overcome the resistant phenotype.

Cross treatment insights: emerging biomarkers and shared regulatory themes

Among all treatment conditions, miR-3191–3p is consistently distinguished between sensitive and resistant cells, by being sharply downregulated in K-562S and strongly induced in K-562R cells. This reproducible pattern positions miR-3191–3p as a promising exosomal biomarker of IM resistance.

The manifested induction of BCL2 targeting miRNAs (miR-34a-5p, miR-1226–3p, miR-204–3p) under different conditions suggests that apoptotic signalling is the most important mechanisms of resensitization, particularly under CBD+IM treatment. Additionally, the exhibited modulation of the metabolic regulators such as miR-103a-3p [53], miR-33a-5p, and miR-33–3p [54] reveals shared but context dependent metabolic rewiring, which is in alignment with the known role of lipid and energy metabolism in CML progression and response to TKI. Overall, the combined data indicate that in the sensitive phenotype, adding CBD to IM enhances apoptotic and differentiation signalling, whereas in the resistant phenotype its therapeutic efficacy is constrained by sustained oncogenic dominance and persistent loss of repressors. These findings highlight the potential of exosomal miRNAs both as biomarkers of resistance and as mediators of treatment-induced cellular adaptation, offering avenues for future functional validation and therapeutic targeting.

Comparative GO enrichment analysis: K-562R vs. K-562S

GO enrichment: conserved regulatory networks and unique lineage-specific difference

Shared functional groups

Consistently enriched functional groups in both cell types and treatments were Transcriptional Regulation, Phosphorylation and Post-translational Modification, Development and Morphogenesis, and Signal Transduction. Respectively, positive regulation of transcription by RNA polymerase II and protein phosphorylation/autophosphorylation were the most overrepresented terms in the compared cell lines. The latter provides evidence for the importance of transcriptional control and kinase-dependent regulatory mechanisms in both phenotypes. In addition, the repeated enrichment of axon guidance and other morphogenetic processes highlight the miRNA-regulated conserved networks that contribute to the developmental plasticity. Importantly, independent of drug treatment, these shared hubs demonstrate that exosomal miRNAs in K-562R and K-562S cells converge on transcription, intracellular signalling, and differentiation programs.

K-562R - specific features.

In resistant cells, the enrichment profile revealed strengthened adaptation to stress and repair processes. IM treatment specifically activated Stress and Cell Fate-related terms, such as cellular response to DNA damage stimulus and DNA repair (RR ~ 0.99), reflecting a DNA surveillance program which was not detected in sensitive cells. CBD treatment in K-562R cells produced an even broader enrichment profile that included Adhesion and Extracellular Interactions, Migration/Motility, and Cytoskeletal Polarity, with maximal enrichment for establishment of cell polarity (RR 1.0). The prominent overrepresentation of neural and synaptic signalling terms propose that resistant cells engage adhesion and neuro-morphogenetic modules to reinforce survival and communication mechanisms. The CBD+IM combination in K-562R produced enrichment of cell differentiation and protein transport, indicating partial re-sensitization via lineage-specific differentiation and vesicle trafficking. Overall, the resistant phenotype was dominated by DNA repair, stress adaptation, and structural remodeling, consistent with mechanisms of drug tolerance.

K-562S-specific features

In addition to the shared hubs, the Imatinib-sensitive cells exhibited a much wider enrichment landscape, encompassing Ion Transport and Homeostasis, Enzyme Activity Regulation, and Adhesion. A substantial number of jointly enriched terms between CBD and IM emerged, encompassing peptidyl serine phosphorylation, actin cytoskeleton organization, angiogenesis, and cell migration. Taken together, these processes highlight a common regulatory impact of both treatments on signalling pathways and cellular motility. In contrast, CBD specific enrichment involved matrix remodeling, synapse assembly, cytoskeletal organization, Wnt signalling, and immune regulation. Collectively, these findings provide strong evidence for CBD's capacity to reshape multiple cellular programs in sensitive cells. Conversely, IM treatment was associated with early adaptive resistance and metabolic shifts, producing a more narrowly focused enrichment profile characterized by cell–cell adhesion, glucose homeostasis, and anti-apoptotic/hypoxia responses. Lastly, CBD+IM combination uniquely enriched positive regulation of excitatory postsynaptic potential and exocytosis, suggesting synergism between the two agents in intracellular communication and vesicle trafficking. Collectively, Imatinib-sensitive cells exhibit pronounced activation of metabolic regulation, cellular

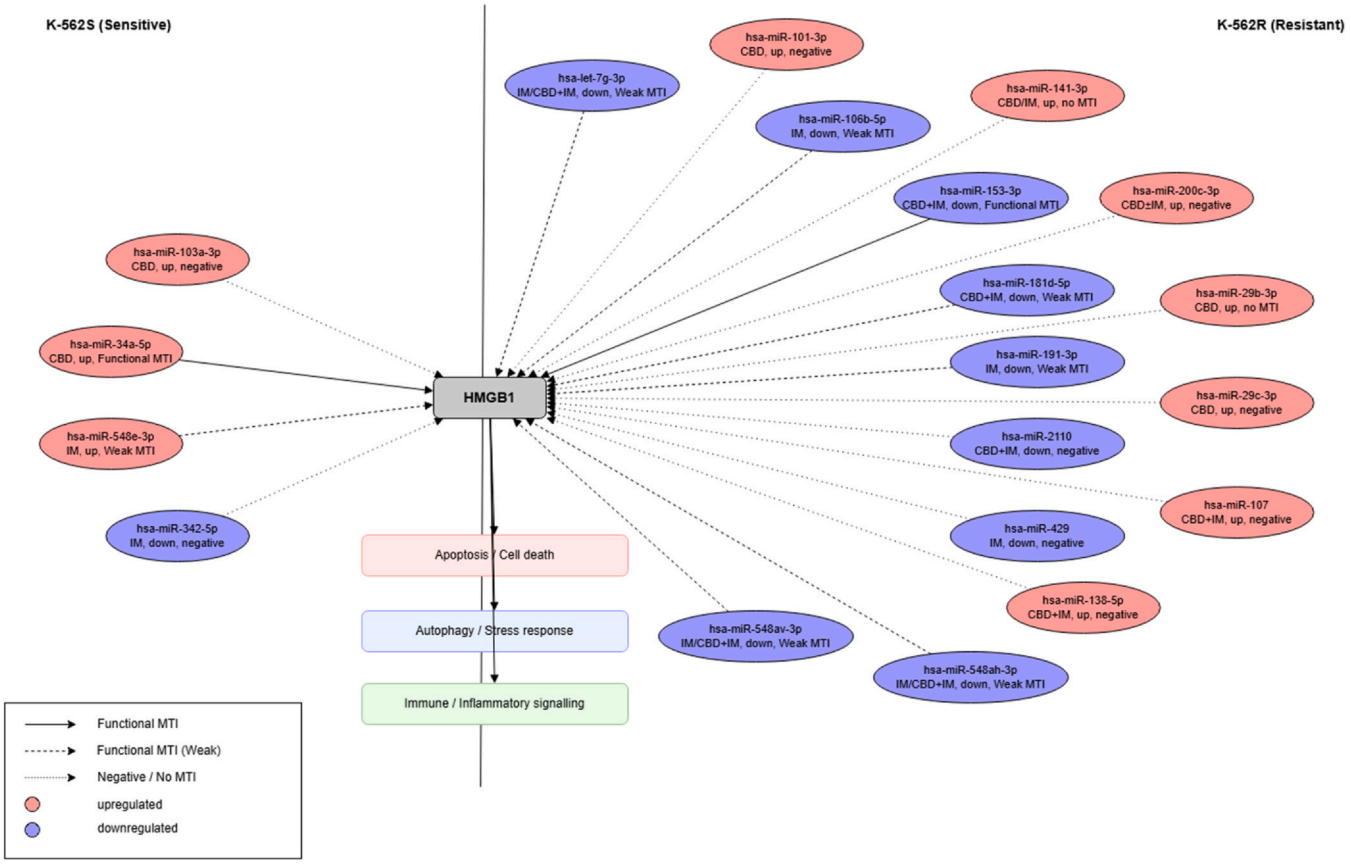

Fig. 14. HMGB1–miRNA regulatory network in K-562S and K-562 R cells. The diagram illustrates the network of differentially expressed miRNAs predicted or validated to target HMGB1 in imatinib-sensitive (K-562S, left semicircle) and imatinib-resistant (K-562 R, right semicircle) chronic myeloid leukemia cells following treatment with CBD, IM, or their combination. Each miRNA is positioned radially around HMGB1 according to phenotype: left semicircle = K-562S, right semicircle = K-562 R. Node color encodes the direction of expression change relative to untreated controls, with red indicating upregulation and blue indicating downregulation. Edges represent miRNA→HMGB1 regulatory interactions and are evidence-coded: solid lines denote Functional MTI (strong experimental support), dashed lines denote Functional MTI (Weak), dotted lines denote negative or unsupported interactions. Functional outcome categories downstream of HMGB1 — Apoptosis/Cell death, Autophagy/Stress response, and Immune/Inflammatory signaling — are shown beneath the central node to contextualize HMGB1's pleiotropic roles. The radial layout highlights phenotype-specific miRNA regulation patterns, including the predominance of downregulated HMGB1-targeting miRNAs in K-562 R cells, and the presence of upregulated miRNAs in K-562S cells, reflecting differential post-transcriptional control of HMGB1 in drug-sensitive versus drug-resistant states.

adhesion, and differentiation, while also preserving the apoptotic and developmental responses.

Interpretive synthesis

Although resistant and sensitive cells share a conserved miRNA-regulated framework involving transcription, signalling, and morphogenetic processes, their treatment-specific enrichments markedly diverge. Resistant cells are primarily dependent on DNA repair and stress adaptation mechanisms, with CBD further stimulating adhesion and polarity programs. In contrast, sensitive cells exhibit much wider regulation involving endocrine, metabolic, and developmental networks, with CBD and IM converging on pathways related to motility, metabolism, and immune signalling. In both phenotypes, the combined treatment triggered vesicle trafficking and differentiation, but in context of resistance, this is a representation of partial re-sensitization, while in sensitive cells it enhances the existing plasticity. Together, these differences illustrate two distinct modes of adaptation shaped by the exosomal miRNAs: resistance imposed by repair-driven resilience, and sensitivity characterized by plasticity-driven responsiveness.

Semantic theme clustering analysis

The semantic theme analysis of exosomal miRNA-target networks revealed fundamentally different organization in resistant (K-562R) and sensitive (K-562S) cells. Dominant interconnected biological themes in K-562R cells were ribosome biogenesis, global transcriptional regulation, and immune/inflammatory signalling. This combination of biosynthetic and immune networks indicates a stress-adaptive response in resistant cells characterized by integration of protein synthesis with transcriptional control and cytokine signalling. Further, the treatment with CBD introduced subnetworks in vesicle trafficking and stress/survival signalling (p53, MAPK, NF-κB, PI3K/AKT), suggesting enhancement of intracellular transport and paracrine communication. In addition, the enrichment of nucleotide catabolism and DNA repair/meiotic recombination following IM exposure reflect activation of genome maintenance and metabolic turnover processes. Lastly, the unique involvement of apoptosis regulation (MOMP) and developmental/regenerative programs by CBD+IM treatment underscores the resilience of the resistant phenotype.

In contrast, the response of K-562S cells was organized around the glial/neural differentiation core hub, which is cross-connected with transcriptional regulation, DNA repair, and immune signalling. This adaptation reveals higher plasticity and developmentally oriented processes, combining lineage-related differentiation with genome maintenance. Treatment with CBD led to enrichment of lipid and sphingolipid metabolism related subnetworks suggesting membrane remodeling and bioactive lipid signalization, while IM enriched RNA metabolism/processing and developmental programs. Conversely, the combination of CBD and IM elicited multifaceted

response (microtubule transport, cell cycle checkpoints, mitotic architecture subnetworks, DNA repair) integrating genome stability with organelle dynamics.

HMGB1-targeting miRNAs

Although most of the HMGB1-associated miRNAs identified in this study have negative multiMiR annotation, several candidates stood out due to their strong differential expression and at least weak functional support (Fig. 14). Importantly, the presence of conflicting evidence for miR-191–3p, miR-548av-3p, miR-548ah-3p, and miR-548e-3p accentuate at the complexity of miRNA-target interactions, which might differ across cellular states, stress conditions, or experimental systems. Of note, miR-153–3p emerged as the only miRNA with clear Functional MTI annotation which together with its marked downregulation in K-562R cells following IM and CBD+IM treatments positions it as compelling candidate for further investigation. Overall, the combination of robust expression changes and weak-to-moderate functional evidence advocate that these miRNAs may have indirect role in HMGB1-related pathways warranting targeted experimental validation.

Conclusions

This study demonstrates exosomal miRNA's capacity to orchestrate distinct adaptive strategies in Imatinib-sensitive and Imatinib-resistant K562 cells. Both phenotypes were found to share conserved regulatory network encompassing transcription, signallig, and morphogenesis. Yet, their responses to treatment differed markedly. In sensitive cells, tumor-suppressive and HMGB1-targeting mRNAs were activated, promoting apoptosis and differentiation, while metabolic and developmental flexibility was largely preserved. In contrast, resistant cells manifested reinforced ribosome-transcription-immune biosynthetic pathways along with activated DNA repair and stress adaptation. Importantly, the HMGB1-targeting miRNAs within miR-584 family were selectively downregulated in K-562R cells. In addition, resistant lineage displayed persistent suppression of miR-615–5p and let-7g-3p, continued downregulation of miR-4435, strong downmodulation of the miR-548 family, and simultaneous upregulation of miR-3191 and miR-33a-5p. Collectively, these miRNAs integrate metabolic reprogramming, stress adaptation, and suppression of apoptotic networks, making them ideal candidate biomarkers of resistance. In combination CBD and IM demonstrated complementary effects: dose minimization through synergistic activation of apoptotic and differentiation pathways in sensitive cells, and consistent chemosensitization in resistant cells that reinstate IM activity while also reduces drug burden. In summary, these experimental observations emphasize the potential of CBD as a therapeutic adjuvant that extends IM's therapeutic window, while also underscoring the critical role of miRNAs as modulators of drug response and resistance.

In essence, treatment sensitivity was defined by adaptive response based on plasticity, whereas resilience to drug exposure was constituted by repair-driven adaptation. Targeting of exosomal miRNA pathways, especially those linked to HMGB1 and resistance-associated networks, may offer new opportunities for overcoming resistance and optimization of combination strategies in leukemia. Of note, due to their stability and accessibility the circulating miRNAs emerge as attractive remote biomarkers for non-invasive diagnostics. The implementation of miRNAs in clinical practice could support translational monitoring of drug response and resistance while simultaneously reducing dependence on ethically challenging animal experimentation.

CRediT authorship contribution statement

Conceptualization, Petar P. Donchev; methodology, Petar P. Donchev; formal analysis, Petar P. Donchev; investigation, Petar P. Donchev; data curation, Petar P. Donchev; writing—original draft preparation, Petar P. Donchev; writing—review and editing, Petar P. Donchev and Prof. Svetla Trifonova Danova; visualization, Petar P. Donchev; supervision, Petar P. Donchev; project administration, Petar P. Donchev; funding acquisition, Petar P. Donchev. All authors have read and agreed to the published version of the manuscript.

Funding

This research was funded by the Bulgarian National Science Fund, grant number КП-06-M61/6.

Data availability

The miRNA sequencing data generated and analyzed in this study are publicly available in the ArrayExpress database (Annotare 2.0, EMBL-EBI) under accession number E-MTAB-16287. Further details can be accessed at https://www.ebi.ac.uk/arrayexpress/.

Declaration of Competing Interest

The authors declare the following financial interests/personal relationships which may be considered as potential competing interests: Petar Petrov Donchev reports financial support was provided by Bulgarian National Science Fund. Petar Petrov Donchev reports a relationship with Stephan Angeloff Institute of Microbiology Bulgarian Academy of Sciences that includes: employment. If there are other authors, they declare that they have no known competing financial interests or personal relationships that could have appeared to influence the work reported in this paper.

Declaration of Generative AI and AI-assisted technologies in the writing process

During the preparation of this work the authors used *Microsoft Copilot (current version, 2025)* in order to assist with data analysis and interpretation. After using this tool, the authors reviewed and edited the content as needed and take full responsibility for the content of the published article.

Acknowledgments

The authors would like to thank the Department of Immunology for accommodating this research and providing valuable support.

The author extends his sincere gratitude to the Bulgarian National Science Fund for the support provided under grant КП-06-M61/6, which was indispensable for carrying out this study.

We thank Assoc. Prof. Emi Haladjova and Prof. Petar Petrov (Institute of Polymers, Bulgarian Academy of Sciences) for their expert support in the DLS verification of exosomes.

Appendix A. Supporting information

Supplementary data associated with this article can be found in the online version at doi:10.1016/j.gmg.2026.100094.

References

[1] M.W. Deininger, J.M. Goldman, J.V. Melo, The molecular biology of chronic myeloid leukemia, Blood 96 (2000) 3343–3356.
[2] J.V. Melo, D.J. Barnes, Chronic myeloid leukaemia as a model of disease evolution in human cancer, Nat. Rev. Cancer 7 (2007) 441–453.
[3] B.J. Druker, F. Guilhot, S.G. O'Brien, et al., Five-year follow-up of patients receiving imatinib for chronic myeloid leukemia, N. Engl. J. Med. 355 (2006) 2408–2417, https://doi.org/10.1056/NEJMoa062867
[4] J.F. Apperley, Part I: Mechanisms of resistance to imatinib in chronic myeloid leukaemia, Lancet Oncol. 8 (2007) 1018–1029, https://doi.org/10.1016/S1470-2045(07)70342-X

[5] N.P. Shah, J.M. Nicoll, B. Nagar, et al., Multiple BCR-ABL kinase domain mutations confer polyclonal resistance to the tyrosine kinase inhibitor imatinib, Cancer Cell 2 (2002) 117–125, https://doi.org/10.1016/S1535-6108(02)00096-X

[6] Y. Hekmatshoar, et al., Exosomes as drug resistance mediators in cancer, Cell Mol. Biol. 64 (2018) 5–13.

[7] F.X. Mahon, M.W. Deininger, B. Schultheis, et al., Selection and characterization of BCR-ABL positive cell lines with differential sensitivity to imatinib, Blood 101 (2003) 2127–2131.

[8] J. Thomas, et al., Detection of BCR-ABL mutations in patients with CML treated with imatinib, Leukemia 18 (2004) 401–408.

[9] K. O'Brien, Exosomal miRNAs in cancer, Cancers 14 (2022) 885, https://doi.org/10.3390/cancers14040885

[10] P. Massi, et al., Cannabidiol as potential anticancer agent, Br. J. Pharm. 168 (2013) 1231–1242, https://doi.org/10.1111/bph.12026

[11] K.A. Scott, et al., Cannabidiol enhances the activity of chemotherapy, Mol. Cancer Ther. 14 (2015) 290–303, https://doi.org/10.1158/1535-7163.MCT-14-0663

[12] A. Shrivastava, et al., Cannabidiol induces programmed cell death in breast cancer cells, Mol. Cancer Ther. 10 (2011) 1379–1390, https://doi.org/10.1158/1535-7163.MCT-11-0188

[13] U. Kosgodage, R. Mould, et al., Cannabidiol (CBD) is a novel inhibitor for exosome and microvesicle release in cancer, Front. Pharm. 9 (2018) 889, https://doi.org/10.3389/fphar.2018.00889

[14] P. Santos, F. Almeida, Exosomal miRNAs as biomarkers in leukemia, Cells 9 (2020) 1450, https://doi.org/10.3390/cells9061450

[15] Q.R. Guo, et al., Exosomal miRNAs in cancer drug resistance, Front. Oncol. 10 (2020) 472, https://doi.org/10.3389/fonc.2020.00472

[16] H. Valadi, K. Ekström, A. Bossios, M. Sjöstrand, J.J. Lee, J.O. Lötvall, Exosome-mediated transfer of mRNAs and microRNAs is a novel mechanism of genetic exchange between cells, Nat. Cell Biol. 9 (2007) 654–659, https://doi.org/10.1038/ncb1596

[17] R. Kalluri, V.S. LeBleu, The biology, function, and biomedical applications of exosomes, Science 367 (2020) eaau6977, https://doi.org/10.1126/science.aau6977

[18] S.P. Da Silva, H.R. Caires, R. Bergantim, J.E. Guimaraes, M.H. Vasconcelos, miRNAs mediated drug resistance in hematological malignancies, Semin. Cancer Biol. 83 (2022) 283–302, https://doi.org/10.1016/j.semcancer.2021.03.015

[19] M.H. Elias, S.F. Syed Mohamad, N. Abdul Hamid, et al., A systematic review of candidate miRNAs, their targeted genes and pathways in chronic myeloid leukemia – an integrated bioinformatical analysis, Front. Oncol. 12 (2022) 848199, https://doi.org/10.3389/fonc.2022.848199

[20] Q.H. Min, et al., Exosomal miRNAs in leukemia progression, Oncol. Rep. 40 (2018) 3505–3513, https://doi.org/10.3892/or.2018.6741

[21] T. Hrdinova, et al., Exosomal miRNAs in hematological malignancies, Int. J. Oncol. 58 (2021) 238–250, https://doi.org/10.3892/ijo.2020.5167

[22] S. Naqvi, et al., Cannabidiol and leukemia drug resistance, *Naunyn-Schmiedeberg's*, Arch. Pharm. (2024).

[23] X. Zhao, et al., Exosomal miRNAs in CML resistance, Front. Oncol. 12 (2022) 848199, https://doi.org/10.3389/fonc.2022.848199

[24] P. Gil-Kulik, N. Kluz, D. Przywara, et al., Potential use of exosomal non-coding microRNAs in leukemia therapy: a systematic review, Cancers (Basel) 16 (2024) 3948, https://doi.org/10.3390/cancers16233948

[25] R. Navakanitworakul, P. Saelue, K. Srinoun, et al., Exosomal miRNA expression profiling in patients with imatinib-resistant chronic myeloid leukemia: A pilot study, PLoS ONE 20 (2025) (eXXXXX).

[26] T. Klumper, H. Bruckmueller, I. Cascorbi, et al., Expression differences of miR-142-5p between treatment-naïve chronic myeloid leukemia patients responding and non-responding to imatinib therapy suggest a link to oncogenic ABL2, SRI, cKIT and MCL1 signaling pathways critical for development of therapy resistance, Exp. Hematol. Oncol. 9 (2020) 15, https://doi.org/10.1186/s40164-020-00174-5

[27] L.H. Shao, L. Zhu, H.L. Li, Mechanisms involved in the HMGB1 modulation of tumor multidrug resistance (Review), Int. J. Mol. Med. 51 (2023) 1–12, https://doi.org/10.3892/ijmm.2023.5272

[28] S. Yuan, Z. Liu, Z. Xu, J. Liu, J. Zhang, High mobility group box 1 (HMGB1): A pivotal regulator of hematopoietic malignancies, J. Hematol. Oncol. 13 (2020) 91, https://doi.org/10.1186/s13045-020-00926-3

[29] Z. Wang, Q. Liu, P. Huang, C. Zhang, Y. Li, et al., miR-299-3p suppresses cell progression and induces apoptosis by downregulating PAX3 in gastric cancer, Open Life Sci. 16 (2021) 266–276, https://doi.org/10.1515/biol-2021-0022

[30] H. Gujrati, S. Ha, M. Waseem, J. Johnson, R. Patel, et al., Downregulation of miR-99b-5p and upregulation of nuclear mTOR cooperatively promotes tumor aggressiveness and drug resistance in African American prostate cancer, Int. J. Mol. Sci. 23 (2022) 9643, https://doi.org/10.3390/ijms23179643

[31] Y. Zhu, H. Tang, L. Zhang, et al., Suppression of miR-21-3p enhances TRAIL mediated apoptosis in liver cancer stem cells by suppressing PI3K/Akt/Bad cascade via regulating PTEN, Cancer Manag. Res. 11 (2019) 955–968, https://doi.org/10.2147/CMAR.S183328

[32] S.M.D. Younis, A. Shareef, L. Baldaniya, et al., The emerging role of miR-362 in cancer: Expression and function across different cancer types, Med. Oncol. 42 (2025) 380, https://doi.org/10.1007/s12032-025-02900-4

[33] A.C. Palcau, C. Pulito, V. De Pascale, et al., CircPVT1 weakens miR-33a-5p unleashing the c-MYC/GLS1 metabolic axis in breast cancer, J. Exp. Clin. Cancer Res. 44 (2025) 100, https://doi.org/10.1186/s13046-025-03355-1

[34] Y.T. Hua, W.X. Xu, H. Li, M. Xia, Emerging roles of miR-133a in human cancers, J. Cancer 12 (2021) 198–206, https://doi.org/10.7150/jca.48769

[35] S. Choi, M.K. Sarker, M.R. Yu, H. Lee, S.H. Kwon, J.S. Jeon, H. Noh, H. Kim, MicroRNA-5010-5p ameliorates high glucose-induced inflammation in renal tubular epithelial cells by modulating PPP2R2D, BMJ Open Diabetes Res. Care 12 (2024) e003784, https://doi.org/10.1136/bmjdrc-2023-003784

[36] A. Altrawy, R.M. Talaat, G.M. Nasr, E.A.E. Badr, R. Arneth, B. Arneth, H. Sabit, Diagnostic and prognostic roles of miR-155 and miR-3173 in breast and ovarian cancer: Implications for early detection and personalized treatment, Biomedicines 13 (2025) 1604, https://doi.org/10.3390/biomedicines13071604

[37] Y. Zhang, H. Liu, X. Li, J. Chen, Q. Wang, et al., miR-1226-5p contributes to radioresistance in colorectal cancer by activating M2 macrophages through suppression of IRF1, J. Transl. Med. 22 (2024) 145, https://doi.org/10.1186/s12967-024-04567-8

[38] A. Xie, H. Wang, J. Huang, M. Sun, L. Chen, miR-3191 promotes the proliferation and metastasis of hepatocellular carcinoma via regulating PAK6, Infect. Agents Cancer 19 (2024) 64, https://doi.org/10.1186/s13027-024-00628-w

[39] M. Abdelkarim, I. Limam, E. Berred, R. Kharrat, B. Sola, F. Ben Aissa Fennira, miR-429 acts as a tumor suppressor in multiple myeloma by regulating cell proliferation, Hemato 6 (2025) 30, https://doi.org/10.3390/hemato6030030

[40] W.M.F.S.B.W. Nor, I. Chung, N.A.B.M. Said, MicroRNA-548m suppresses cell migration and invasion by targeting aryl hydrocarbon receptor in breast cancer cells, Oncol. Res. 28 (2021) 615–629, https://doi.org/10.3727/096504020X16037933185170

[41] F. Biamonte, G. Santamaria, A. Sacco, F.M. Perrone, A. Di Cello, A.M. Battaglia, A. Salatino, A. Di Vito, I. Aversa, R. Venturella, F. Zullo, F. Costanzo, MicroRNA let-7g acts as tumor suppressor and predictive biomarker for chemoresistance in human epithelial ovarian cancer, Sci. Rep. 9 (2019) 5668, https://doi.org/10.1038/s41598-019-42221-x

[42] S. Dai, F. Li, S. Xu, J. Hu, L. Gao, The important role of miR-1-3p in cancers, J. Transl. Med. 21 (2023) 769, https://doi.org/10.1186/s12967-023-04649-8

[43] Y.T. Hua, W.X. Xu, H. Li, M. Xia, Emerging roles of miR-133a in human cancers, J. Cancer 12 (2021) 198–206, https://doi.org/10.7150/jca.48769

[44] M. Gharipour, M. Sadeghi, Pivotal role of microRNA-33 in metabolic syndrome: A systematic review, ARYA Atheroscler. 9 (2013) 372–376.

[45] J.W. Hong, J.M. Kim, J.E. Kim, H. Cho, D. Kim, W. Kim, J.W. Oh, H.J. Kwon, MiR-4435 is a UQCRB-related circulating miRNA in human colorectal cancer, Sci. Rep. 10 (2020) 59610, https://doi.org/10.1038/s41598-020-59610-2

[46] Y. Kuwano, K. Nishida, K. Kajita, et al., Transformer 2β and miR-204 regulate apoptosis through competitive binding to the 3′UTR of BCL2 mRNA, Cell Death Differ. 22 (2015) 815–825, https://doi.org/10.1038/cdd.2014.176

[47] Z. Mohamadzade, B.M. Soltani, Z. Ghaemi, P. Hoseinpour, Cell-specific tumor suppressor effect of hsa-miR-1226-3p through downregulation of HER2, PIK3R2, and AKT1 genes, Int. J. Biochem. Cell Biol. 134 (2021) 105965, https://doi.org/10.1016/j.biocel.2021.105965

[48] X. Gao, X. Fan, W. Zeng, J. Liang, N. Guo, X. Yang, Y. Zhao, Overexpression of microRNA-107 suppressed proliferation, migration, invasion, and the PI3K/Akt signaling pathway and induced apoptosis in hypopharyngeal squamous cell carcinoma, Bioengineered 13 (2022) 7880–7892, https://doi.org/10.1080/21655979.2022.2051266

[49] N. Song, P. Li, P. Song, et al., MicroRNA-138-5p suppresses non-small cell lung cancer cells by targeting PD-L1/PD-1 to regulate tumor microenvironment, Front. Cell Dev. Biol. 8 (2020) 540, https://doi.org/10.3389/fcell.2020.00540

[50] M.V. Singh, K. Dhanabalan, J. Verry, A.O. Dokun, MicroRNA regulation of BAG3, Exp. Biol. Med. 247 (2022) 617–623, https://doi.org/10.1177/15353702211066908

[51] A comprehensive review on miR-153: Mechanistic and controversial roles of miR-153 in tumorigenicity of cancer cells, Front. Oncol. 12 (2022) 985897, https://doi.org/10.3389/fonc.2022.985897

[52] M. Xu, J. Zhou, Q. Zhang, K. Le, Z. Xi, P. Yi, X. Zhao, J. Tan, T. Huang, MiR-3121-3p promotes tumor invasion and metastasis by suppressing Rap1GAP in papillary thyroid cancer in vitro, Ann. Transl. Med. 8 (2020) 1229, https://doi.org/10.21037/atm-20-4469

[53] Z. Sun, Q. Zhang, W. Yuan, X. Li, C. Chen, Y. Guo, B. Shao, Q. Dang, Q. Zhou, Q. Wang, G. Wang, J. Liu, Q. Kan, MiR-103a-3p promotes tumour glycolysis in colorectal cancer via Hippo/YAP1/HIF1A axis, J. Exp. Clin. Cancer Res. 39 (2020) 250, https://doi.org/10.1186/s13046-020-01705-9

[54] R. Ortega, B. Liu, S.J. Persaud, Effects of miR-33 deficiency on metabolic and cardiovascular diseases: Implications for therapeutic intervention, Int. J. Mol. Sci. 24 (2023) 10777, https://doi.org/10.3390/ijms241310777